磁性細菌Magnetospirillum magnetotacticum MS-1により合成されたマグネタイトの磁気特性についての研究

Study on the magnetic properties of magnetite synthesized by *Magnetospirillum Magnetotacticum* MS-1

By

YIRILETU

A THESIS SUBMITTED TO THE
MURORAN INSITUTITE OF TECHNONLGY
FOR THE DEGREE OF
DOCTOR OF PHILOSOPHY
IN THE
DIVIDION OF ENGINEERING FOR COMPOSIT FUNCTION

MARCH/2016

ABSTRACT

Magnetotactic bacterium (MTB) is a class of bacterium which tends to move in response to the environment's geomagnetic lines. MTB forms magnetic nanoparticles (MNPs: *e.g*. magnetite Fe_3O_4 or greigite Fe_3S_4) with a size of 35-120 nm *in vivo*. Each of MNPs is surrounded by a phospholipid bilayer. They form a chain structure composed of 15-20 MNPs, which is called “magnetosome”. The first MTB strain isolated and cultured was *Magnetospirillum magnetotacticum* MS-1, which produces highly pure Fe_3O_4 crystals with a single magnetic domain. My doctoral thesis is a summary of an investigation of the magnetic properties of magnetite synthesized by MTB strain MS-1 cells grown with different concentrations of ferric (Fe^{3+}) iron or with different conditions of transition metal element (Fe/Zn/Co). The results were as follows:

The total yield of magnetic cells of MS-1 increased with the increase of the initial Fe^{3+} concentrations, even though the total yield of the MS-1 cells was independent on the initial Fe^{3+} concentrations. The maximum coercivity (H_c) and saturation magnetization (M_s) values were observed at Fe^{3+} concentration of 34 μM. The relationship between Verwey transition temperature (T_V) and Blocking temperature (T_B) ($T_V < T_B$) of dried cells suggested that MNPs were arranged in chain when MS-1 cells were grown with the different initial Fe^{3+} concentration. The above results illustrated that the initial Fe^{3+} concentration had a marginal effect on the magnetic properties of MTB strain MS-1, except for the medium without addition of Fe^{3+}.

In the growth medium (GM) containing transition metal element (Fe/Zn/Co), the growth rate of MS-1 cells was not significantly different. The size of magnetosome became smaller in the GM with Fe/Zn or Fe/Co than that in the GM with Fe. The change in M_s, H_c, T_V, T_B suggested that the magnetic properties of intact cell (IC), magnetosome (MG) and magnetite (MT) was influenced by Zn or Co. In the GM with Fe/Zn, the M_s value of IC, MG and MT was decreased. H_c value of IC and MG was not significantly different with Fe culture, but that of MT was increased. Also, the T_V was not significantly different from that of the GM with Fe in IC, MG and MT, but the T_B value of IC and MG was increased. The T_B of MT unchanged. In the GM with Fe/Co, the H_c value of IC, MG and MT increased and M_s in IC or MG decreased. M_s value of MT was not significantly different from the value of Fe. T_V and T_B were not detected.

論文内容の要旨

磁性細菌（magnetotactic bacteria, MTB）は、環境の地磁気線に応じて移動する細菌である。MTB の菌体内で大きさが 35～120 nm の磁性ナノ粒子（magnetic nanoparticles, MNPs；マグネタイト（Fe_3O_4）またはグレガイト（Fe_3S_4）が形成される。MNPs のそれぞれは、リン脂質二重層に囲まれていて 15～20 個並んだ「マグネトソーム（magnetosome）」と呼ばれるチェーン構造を形成している。初期に単離培養された MTB は *Magnetospirillum magnetotacticum* MS-1 で、単磁区で高純度の Fe_3O_4 の結晶を生成する。本博士論文は、異なる Fe^{3+}の濃度及び異なる遷移金属元素（Fe/Zn/Co）を含む培地で培養した MTB 株 MS-1 で合成されるマグネタイトの磁気特性を MPMS で調べたものである。主要な結果は以下のどおりである。

まず、異なる Fe^{3+}の濃度の影響について述べる。MS-1 細胞の総量は培地中の初期 Fe^{3+}の濃度と関係がなかったが、Fe^{3+}の濃度が上がるにつれ、磁石に引きつけられる細胞の量が多くなることが分かった。培地中の Fe^{3+}が 34 μM のとき、保磁力（H_c）と飽和磁化（M_s）の最大値が観察された。Verwey 転移温度（T_V）とブロッキング温度（T_B）（$T_V < T_B$）との関係は、培地中の初期の Fe^{3+}濃度と関係なく、MS-1 細胞の増加に伴い、MNP がチェーン状に配置されていることを示唆している。これらの結果は、マグネタイトの磁気特性は培地中の Fe^{3+}の濃度にわずかであるが影響されることを示唆する。

次に、異なる遷移金属元素（Fe/Zn/Co）を含む培地を用いた結果について述べる。MS-1 細胞の成長速度は培地中の Fe、Zn あるいは Co に影響されないが、合成されるマグネトソームのサイズが Zn 或は Co 培地では小さくなる。H_c、M_s、T_V、T_B 値の変化から見て、細胞全体（IC）、マグネトソーム（MG）とマグ

ネタイト（MT）における磁気特性が Zn 或は Co に影響されることが分かった。Zn を含む培地では、IC、MG と MT の M_s 値が低下する。そして、IC と MG の H_c 値が標準 Fe のそれと比べ有意差がなかったが、MT の H_c 値が大きくなった。また、標準 Fe の T_V と比べて、IC、MG と MT の T_V 値には変化がなかったが、IC、MG の T_B 値は大きくなった。MT の T_B には変化がなかった。Co を含む培地では、標準 Fe の H_c と比べて IC、MG と MT における H_c 値が大きくなった。M_s 値が IC、MG で低下したが、MT では大きな変化がなかった。また、T_V と T_B 値はどちらの培地でも検出できなかった。以上の結果は、培地中の Co や Zn がマグネタイト中に微量取り込まれたことを示唆していると考えられる。

Abbreviations

MTB	magnetotactic bacteria
MS-1	*Magnetospirillum magnetotacticum* strain MS-1
AMB-1	*Magnetospirillum magneticum* strain AMB-1
MSR-1	*Magnetospirillum gryphiswaldense* strain MSR-1
RS-1	*Desulfovibrio magneticus* strain RS-1
MC-1	*Marine coccus* strain MC-1
MV-1,2,4	*Magnetic vibrio* strain MV-1 (or -2 or -4)
H_c	coercivity
H_r	remanence coercivity
M_s	saturation magnetization
M_r	remanence magnetization
T_B	Blocking temperature
T_V	Verwey transition temperature
FC	field cooled
ZFC	zero field cooled
TEM	transmission electron microscope
MPMS	magnetic property measurement system
EPMA	electron probe microanalysis

Chapter 1 Introduction

Magnetic materials have a wide variety of unique property and applications. Recently many researchers are interested in the study of magnetic nanoparticles (MNPs). The MNPs were developed in recent years from ordinary nanoparticles such as the small size effect, interface effect, quantum effect and quantum tunnel effect. Moreover, MNPs also have unique magnetic properties such as superparamagnetism (SPM), high coercivity (H_c), and high susceptibility, and are easily separated from the reaction system, and recovery features. Their application fields have been widely expanded in clinical diagnosis, targeted drugs, biological sensor, immobilized enzyme and wastewater treatment *etc*.[1] So, the researchers are focused on obtaining MNPs more preferably through improved production method; it is called artificially synthesized method. However, the artificially synthesized MNPs have some drawback: (1) lower purity; (2) grain size too small (< 20 nm) and easily cluster; (3) low coupling ability between nanoparticles and bio-molecule or medicine. Therefore, the biomineralization progress is attention by researchers.

1.1 Magnetotactic bacteria (MTB)

Magnetotactic bacteria (MTB) are a special microorganism which can take up the iron ions from the environment and form highly pure crystal of magnetite (Fe_3O_4)[2] and/or greigite (Fe_3S_4)[3-5] *in vivo*. The crystals of Fe_3O_4 (or Fe_3S_4) are

surrounded with 3-4 nm of phospholipid bilayer, and they are arranged in a chain structure in the bacterial cell, which is called “magnetosome” (Fig. 1a)[6, 7]. The “magnetotaxis” movement of MTB is to rely on the magnetosome and flagellum[8]: MTB contain magnetosome as the “magnetic needle” *in vivo*, which mediated MTB magnetic movement; MTB, by rotating flagella, promote their swimming in the water (Fig. 1b). MTB migrates along geomagnetic field (B_{geo}) lines and negative tactic response to oxygen (O_2) (Fig. 2)[7]. MTB swim preferentially parallel to the B_{geo} and migrate northward (tendency of magnetic S pole) at the northern hemisphere (NH), they have north polarity, which is called “North-seeking (NS)”. Otherwise, at the southern hemisphere (SH), MTB swim preferentially antiparallel to the B_{geo} and migrate southward (tendency of magnetic N pole), they have south polarity, which is called “South-seeking (SS)”. NS and SS cells are appeared in the near the equator at the same time, the proportion of the NS cells are increased in the NH; conversely, the number of SS cells is increased.[7]

A variety of MTB is widely distributed throughout the natural environment such as freshwater or mud interface of the marine conditions, the chemical gradient stratification of the aquatic environment and marine waters of an oxic-anoxic transition zone (OATZ). Type and quantity of MTB are affected on the OATZ location and other nutrients such as soluble iron, sulfide *etc*. In general case, the concentration of the dissolved oxygen decreased and the concentration of the solubilized sulfur increased with increasing the water depth. Therefore, MTB are mostly microaerobic or anaerobic bacteria in freshwater or sediments conditions, which synthesize Fe_3O_4 and Fe_3S_4 *in vivo* within the OATZ

upper and lower, respectively. [8]

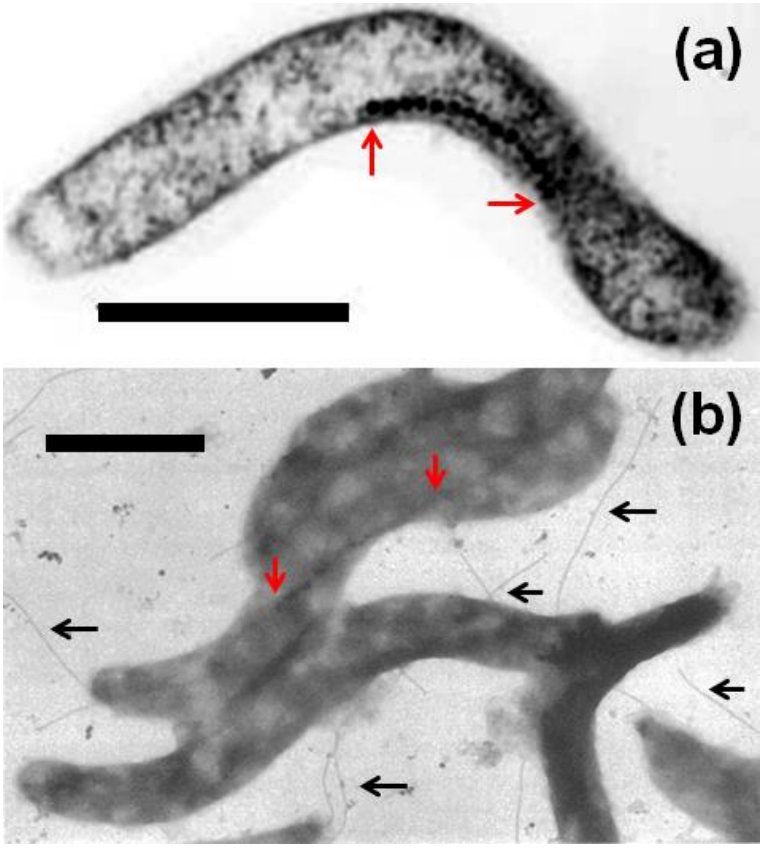

Fig. 1 TEM (a) and EM (b) image of a typical intact cell of the *Magnetospirillum magnetotacticum* (MS-1) by Dr. Shimazaki Y. (a) and Blakemore (b)[8]. A chain of magnetosomes and flagella are shown by red and black arrows, respectively. The scale bar was 1 μm in each figure.

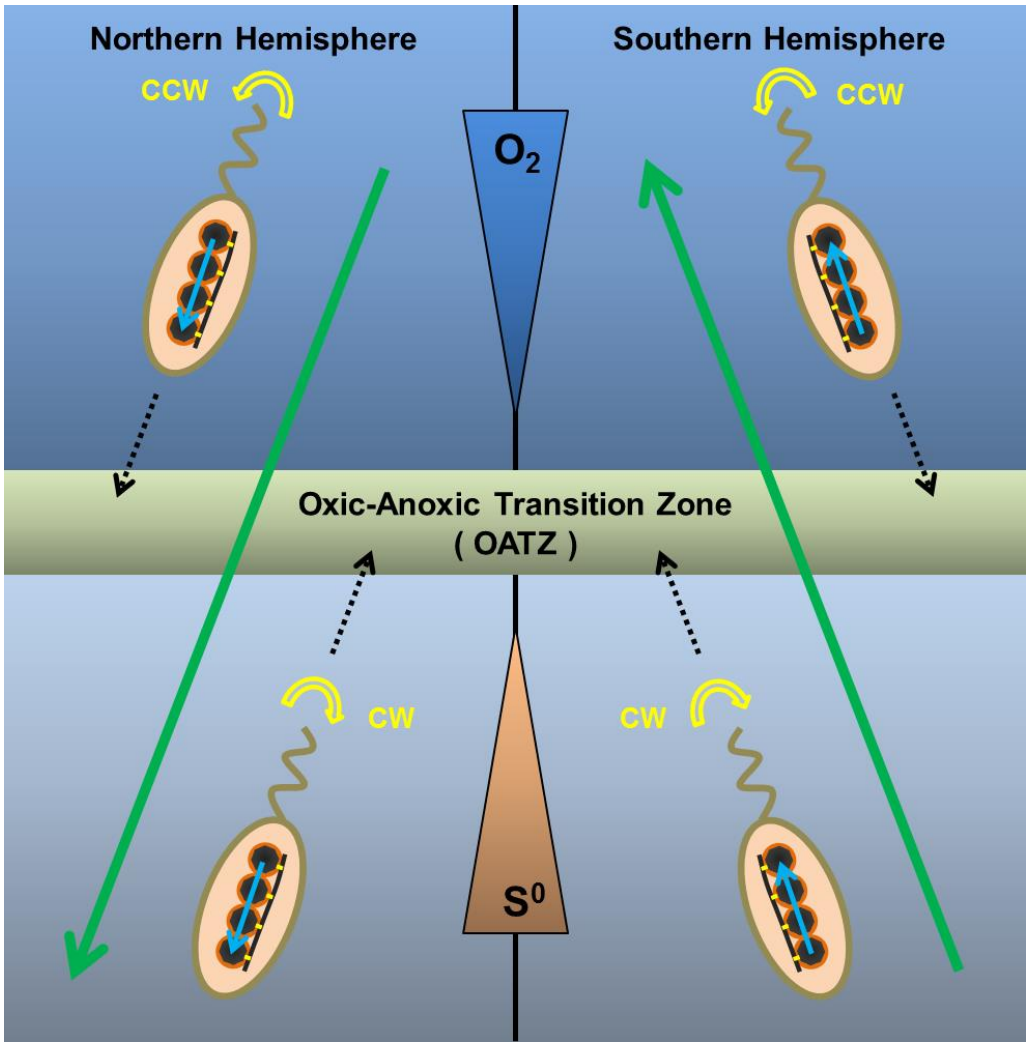

Fig. 2 Hypothetical model of the moving behavior of magnetotactic bacteria (MTB) in the Northern (NH) or Southern (SH) hemisphere. The cells efficiently seek their optimum oxygen concentration (O_2) at the microaerobic oxic-anoxic transition zone (OATZ) in water column or sediment conditions. Cells on the oxic (or anoxic) side of the OATZ swim downward (or upward) (dotted black arrows) by rotating their flagella counterclockwise (CCW) (or clockwise (CW)) (open yellow arrows) along the geomagnetic field (B_{geo}; green arrows) in NH and SH hemispheres, and the magnetic dipole moment (blue arrows) of cell's is opposite direction in NH and SH hemispheres.

1.1.1 Discovery of MTB

Magnetotactic bacteria (MTB) have been mentioned in an unpublished manuscripts by Bellini who has examined the magnetosensitive bacteria in aquatic bacteria at first[9]. He found some microorganism moved along the B_{geo} when he tested water samples from sources around Pavia for pathogens by using microscopy. He observed that dead cells did not migrate along the applied magnetic field direction in the water drops, but it oriented in the same direction; when a bar magnet or small electromagnets could exceed the B_{geo}. This behavior was called “magneto-sensitivity” by the researcher. However, this study did not get attention.

Blakemore was the first American biological scientist who reported the MTB on the journal “Science” in 1975[10]. He collected the spirillum that forms at the surface sediments of the salt marshes of Cape Cod, Massachusetts, and from the surface layers of sedimentary cores of a depth from 15 m in Buzzards Bay. A class of microorganisms always migrated in the northern edge of the field of a microscope when he observed the drop of mud sample under the microscopy. This class of microorganism was called “magnetotactic bacteria (MTB)”, and this behavior was called “magnetotaxis.” He obtained purified MTB suspensions and measured by using the electron microscopic. He discovered that the MTB have two bundles of flagella at one side of the cell and they have two chains which containing approximately 5-10 crystal-like particles *in vivo*. [10] He detected iron (Fe) was the predominant element within the crystal-like particles by using energy dispersive x-ray microanalysis (EDXMA). According to this study, they isolated and cultured MTB strain MS-1 at first, and also is originally named as

"*Aquaspirillum magnetotacticum* strain MS-1"[6], later that is called as "*Magnetospirillum magnetotacticum* strain MS-1"[8] (Fig. 3a).

1.1.2 Varieties and characteristics of MTB

Since the first MTB was reported by Blackmore, the various biological scientists isolated nearly 30 different types of MTB from different environment such as ocean, lake or sediment by using the different methods, for example, determination of the 16S rRNA sequence, fluorescence labeling *etc*. They represent various cellular morphologies as spirillum, vibrio, coccus, rod-shaped and multicellular bacteria (Fig. 3). However, pure cultures of the strain under the laboratory conditions were not many, such as *Magnetospirillum* (*M.*) *magnetotacticum* MS-1, *M. magneticum* AMB-1[11], *M. gryphiswaldense* MSR-1[12], *Desulfovibrio magneticus* RS-1[13], *Marine coccus* MC-1[14] and *Magnetic vibrio* MV (-1, -2, -4)[15, 16] *etc*. Among them, the MS-1, AMB-1 and MSR-1 are often used as a model strain in the study.

Although MTB have variety of types and morphologies, but researchers found these bacteria have common characteristics as following: (1) they belong to the gram-negative bacterium; (2) swim by using rotating flagella; (3) show a negative tactic response to the atmospheric concentrations of oxygen; (4) the optimal pH and temperature are 6-7 and nearly 30 °C, respectively; (5) cells contain a variable number of magnetosomes, which are arranged one or more columns along the zone axis of the cells or are arranged at the both ends of the

zone axis of the cells or random arrangement *in vivo*.

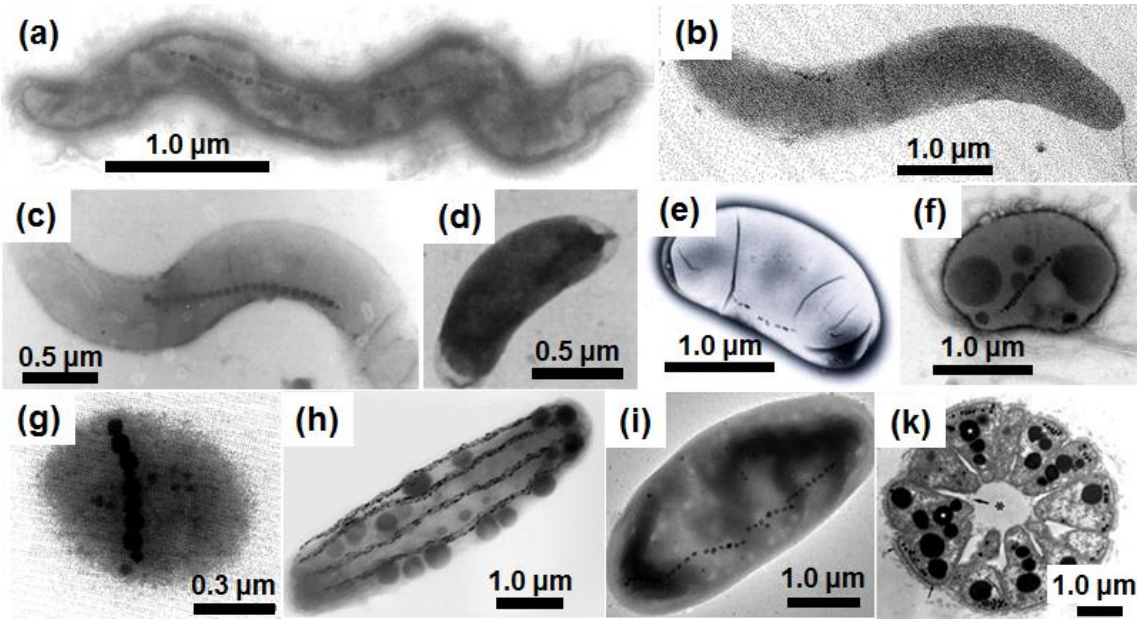

Fig. 3 Transmission electron micrograph (TEM) or electron micrograph (EM) of various morphology of magnetotactic bacteria (MTB): spirillum: a-c; vibrio: d and e; coccus: f and g; rod-shaped: h and I; and multicellular bacterium: k.[8, 17-21]

1.2 Magnetosome

MTB contain several MNPs which are surrounded with 3-4 nm of phospholipid bilayer. Such MNPs are called magnetosome (Fig. 4)[6]. The morphology, magnetosome crystal type, chemical composition and arrangement different within the cell of the isolated MTB from the different environment are considerably difference.

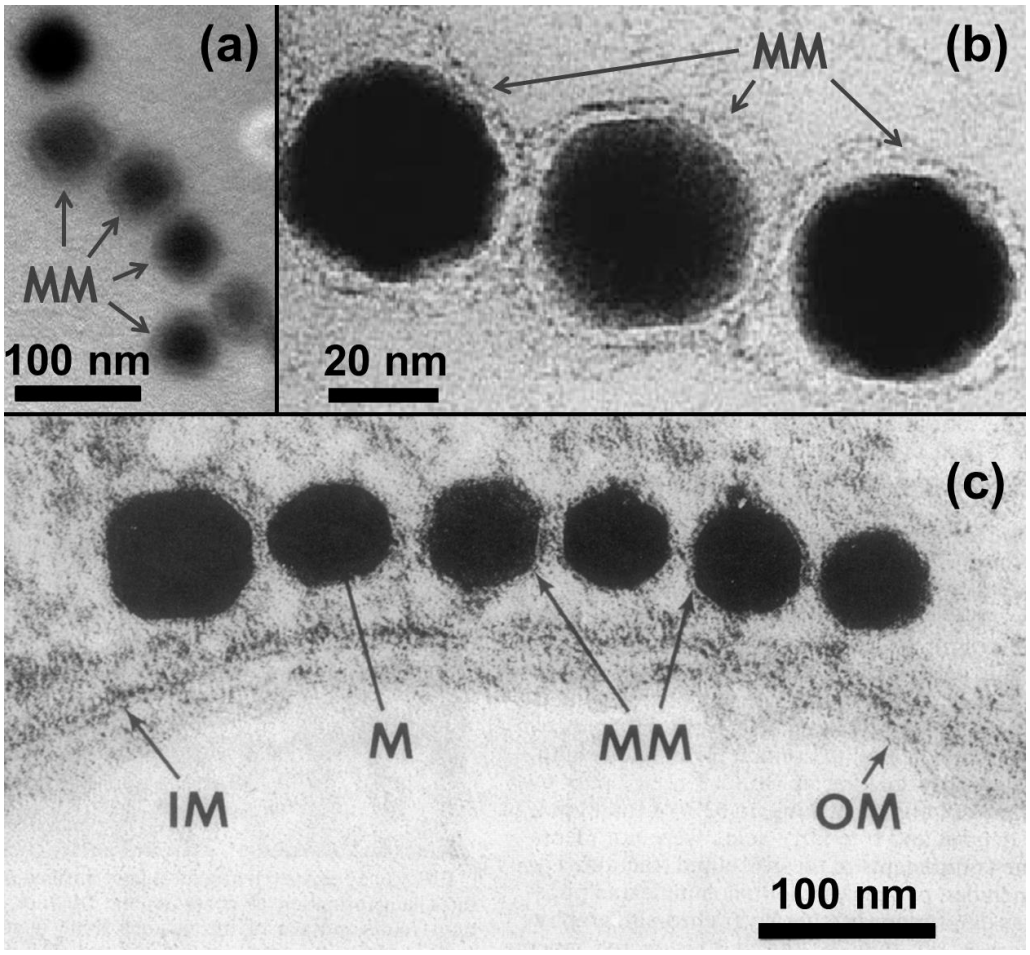

Fig. 4 TEM image of a magnetosomes in *M. magnetotacticum* (MS-1; (a): our study; and (c)[6] and *M. gryphiswaldense* (MSR-1; (b)[22]. The magnetosome membrane (MM), outer membrane (OM), inner membrane (IM) and magnetite (M) are indicated by arrows.

1.2.1 Chemical composition and morphology of magnetosome

The chemical composition of the magnetosome of MTB is iron oxides or iron sulfide. Most magnetosome contains magnetite (Fe_3O_4)[2]; the magnetosome in the few MTB formed iron sulfide under the marine or sulfur-rich conditions, such as greigite (Fe_3S_4)[3, 4], mackinawite (FeS)[7]; Bazylinski *et al*.[7] speculated that

FeS was the precursor of Fe_3S_4; Farina *et al*.[5] found the monocrystalline pyrrhotite (Fe_7S_8) and non-magnetic pyrite (FeS_2) particles within the prokaryotic microorganisms *in vivo*; an irregular of coccus contained both iron oxides and iron sulfide in magnetosome. However, the strain was not cannot be pure cultured[23].

MTB contain highly pure MNPs, but a small amount of impure crystal doped other metal element such as titanium (Ti), copper (Cu), zinc (Zn), manganese (Mn) and cobalt (Co) *etc*. were reported in a few strains of uncultured MTB: Towe *et al*.[24] detected a trace of Ti element in the magnetosome of the spherical MTB which lived in freshwater; Bazylinski *et al*.[25] found the isolated magnetotactic prokaryote have iron sulfide magnetosome that contained a large amount of Cu which ranged from about 0.1 to 10 atomic percent relative to Fe, mostly presented in magnetosome surface; Zn and Mn element were detected in the analyzed magnetosome[26]; the magnetosome of the isolated MTB strain YSC-1 contained Fe element (52.9%), but also contained Co element (45.4%) reported by Gao *et al*.[27]. These reports show: the mineralization within living cells are highly influenced by ambient environmental chemical conditions, resulted in the magnetosome incorporation of other metallic element in the growth process of MTB.

MNPs are surrounded by a thin layer of lipid bilayer membrane *in vivo*, that controls the grain size and shape of MNPs crystal. The result of magnetosome lipid analysis shows: magnetosome membrane contains protein, fatty acid, glycolipids, sulfatide, phospholipids and other organic ingredient[6]. The surface of magnetosome membrane has a functional groups which mainly include the

carboxyl, hydroxyl and amino[28]. The protein was not detected in magnetosome crystals[29].

MTB synthetic magnetosome has species' or strain-specific shapes (Fig. 5). Fe_3O_4 types of magnetosome have three morphologies: cubo-octahedral, elongated hexagonal prismatic, and bullet-shaped. The magnetosome contains the cubo-octahedral MNPs in the model MTB (MS-1, AMB-1 and MSR-1). Comparison with the artificially synthesized MNPs, the Fe_3O_4 magnetosome of MTB has a prefect crystal structure. Many researchers consider it as the standard of ideal crystalline[16, 30].

Although the morphology of magnetosome diverse, they have common characteristics as follows: (1) Chemical composition is pure. The magnetosome mainly contain Fe_3O_4 or Fe_3S_4. (2) Particle is narrow size distribution and uniform. The size is typically ranged 35-120 nm. (3) Each particle is surrounded by a lipid bilayer membrane. (4) Magnetosomes are arranged in chain structure and it is along with the major axis of cells.

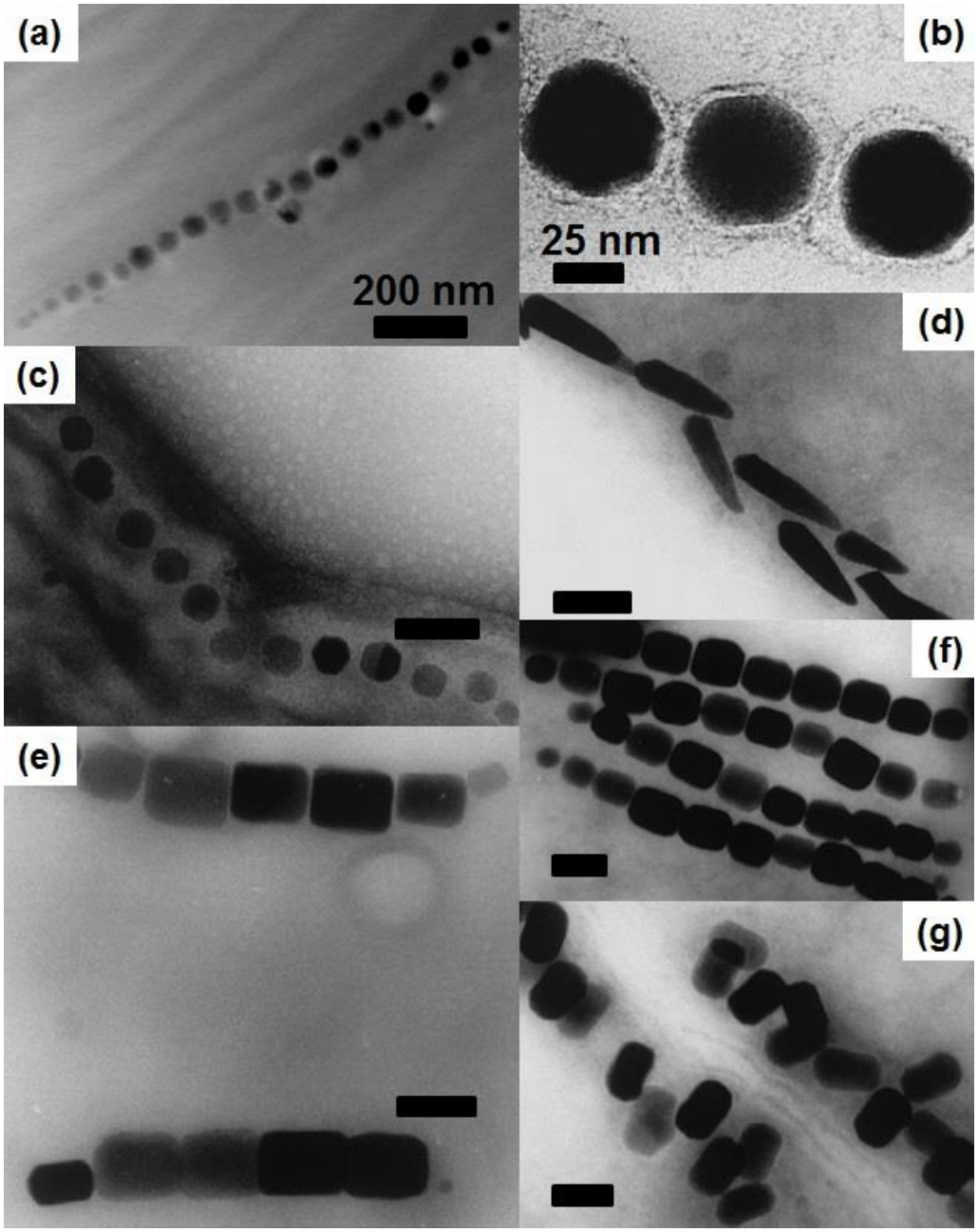

Fig. 5 Morphology and arrangements of magnetosome in various MTB. Characteristic crystal habits found in MTB are cubo-octahedral (a-c), bullet-shaped (d), and elongated hexagonal prismatic morphologies (e-g). Crystals can be arranged in single (a-d) or two (e) or multiple chains (f) or irregular (g) *in vivo*. Scale bar was marked in (a), and (b); those in (c-g) are equivalent to 100 nm. Figure (a) provided by our study, figure (b-g) reproduced from Schüler and Frankel[22].

1.2.2 The factors influence the magnetosome formation

MTB lives in OATZ, can absorb Fe ion from the environment and form the MNPs *in vivo*. Therefore, oxygen and iron are key factors for magnetosome formation.

1.2.2.1 Oxygen affect magnetosome formation

The cultured MTB usually grew under anaerobic-microaerobic conditions, so the oxygen concentration influences on the magnetosome formation. Blakemore *et al*.[31] showed that the optimal O_2 concentration for magnetosome formation in MTB strain MS-1 was 1%, and that magnetosome formation was inhibited when the O_2 concentration was more than 5%. The O_2 concentration of magnetosome formation in MTB strain MSR-1 will need to the controlled within the narrow range: the magnetosome is formed normally below the O_2 concentration of 20 mbar and the formation is maximum at 0.25 mbar dissolved oxygen tension[32]. Yang *et al*.[33] indicated that the trace oxygen (2-14% in the gas phase or < 0.20 ppm in the liquid phase) enhanced cells growth with increasing the number of magnetosome when MTB strain AMB-1 grew in different O_2 concentrations. They found that number of the magnetosome began to decrease, when O_2 exceeded 15% (0.20 ppm in liquid phase) and the magnetosome formation was almost completely inhibited when O_2 was more than 35% (> 0.40 ppm in liquid phase). The maximum magnetosome production was observed at 2.35 μM O_2, and the magnetosome formation was partly inhibited at 11.7 μM O_2. It was totally

inhibited at 23.52 μM O_2[34].

Among several strains of MTB shown above, MSR-1 provided the maximum yield of magnetosome[35-37]: Blakemore *et al*.[8] reported the wet weight of cells was 0.2-0.5 g/L at 0.6-1.0% of oxygen (gas phase); Heyen and Schüler[35] reported 0.4 g/L cells can produce approximately 6.0 mg/L/d magnetosome (the dry weight of magnetosome production per one Liter growth medium per day) under optimal conditions; Sun *et al*.[36] obtained the highest yield of cells (2.17 g/L) and magnetosome production (16.7 mg/L/d) by using the 42-L fermentor under the optimal oxygen condition. Naresh *et al*.[37] presented the cells yield and magnetosome production by controlling dissolved oxygen was kept at 6% by devising a 3-L bioreactors to achieved approximately 1.5 g/L and 9.0 mg/L/d, respectively. Mandernack *et al*.[38], however, used oxygen isotope analysis to show that the oxygen in Fe_3O_4 was derived from H_2O, indicating that O_2 was not directly involved in the synthesis of Fe_3O_4. Thus, the mechanism by which O_2 concentration affects magnetosome formation remains unclear, as mentioned by Heyen and Schüler[35].

1.2.2.2 Iron affect magnetosome formation

Another key factor - iron is an essential inorganic element for cell growth and magnetosome formation. Many proteins such as cytochrome, superoxide dismutase (SOD) and nitrogenase *etc*. contains Fe in cell body. The MTB contain high concentration of Fe *in vivo*, in addition to proteins contain Fe, and

the magnetosome is mainly composed of Fe. The content of Fe achieved or exceeded 2% of the dry weight of cells; it was 100 times larger than that of the *E. coli* (0.013-0.014%)[8, 39]. Therefore, the concentration of iron in growth medium necessary effects the MTB growth and magnetosome formation[40, 41].

Generally, the source of iron in the growth medium usually used ferric iron chelator such as Fe-quinate or Fe-citrate. Schüler *et al*.[42] indicated the utilization ability of Fe^{3+} was higher than Fe^{2+} in MSR-1 cells, yet Fe^{3+} was low solubility and easy to precipitate at alkaline condition, the compounds of chelator are not used better by the MTB, however, they utilized Fe salt to produce amount of magnetosome at same condition. Comparison of the magnetosome production of AMB-1 grown in several ferric chelate and ferrous sulfate, the Fe^{2+} can promoted the magnetosome formation that is greatly increased by ferrous sulfate and ferric gallate, and it was significantly higher than Fe-quinate[33].

The magnetosome formation is closely related to iron concentrations in the growth medium which is containing commonly 20-40 μM of Fe-quinate or 50-100 μM of Fe-citrate. Schüler [42] deemed the Fe utilization of cells achieved to saturation at 15-20 μM. The magnetosome production is not obviously increased when iron concentrations exceeded 20 μM, while that of higher than 200 μM were cell growth inhibiting.

1.2.3 Mechanism of magnetosome formation

Although the formation mechanism of magnetosome is still not completely

demonstrated in detail, through various hypothetical models on the formation mechanism, the formation process are thought to be including as following steps: at first, MTB absorb the Fe ion from the environment; then, Fe ion transport in to the magnetosome vesicle; and biologically formed Fe_3O_4 or Fe_3S_4 within the magnetosome vesicle finally.

Frankel *et al*.[43] proposed the model of magnetosome formation in MS-1 based on the results of Mössbauer spectroscopy: MS-1 cells absorb Fe^{3+} and reduced it to Fe^{2+}. Fe^{2+} was transported into the magnetosome vesicle, and then Fe^{2+} was oxidized again and formed $Fe_2O_3 \cdot nH_2O$, and one-third of Fe^{3+} is reduced, further $Fe_2O_3 \cdot nH_2O$ dehydrated and finally formed Fe_3O_4. MTB strain MV-1 contained $Fe_2O_3 \cdot nH_2O$ by using Mössbauer spectroscopy[15]. Schüler and Baeuerlein[32] indicated the iron absorption and magnetosome formation was closely related, there was no obvious accumulation of the Fe_3O_4 premise product in MSR-1. Schüler[17] summarized the model of magnetosome formation in *Magnetospirillum* species and showed in Fig. 6. Bazylinski and Frankel[7] proposed a more refined model of magnetosome formation and showed in Fig. 7.

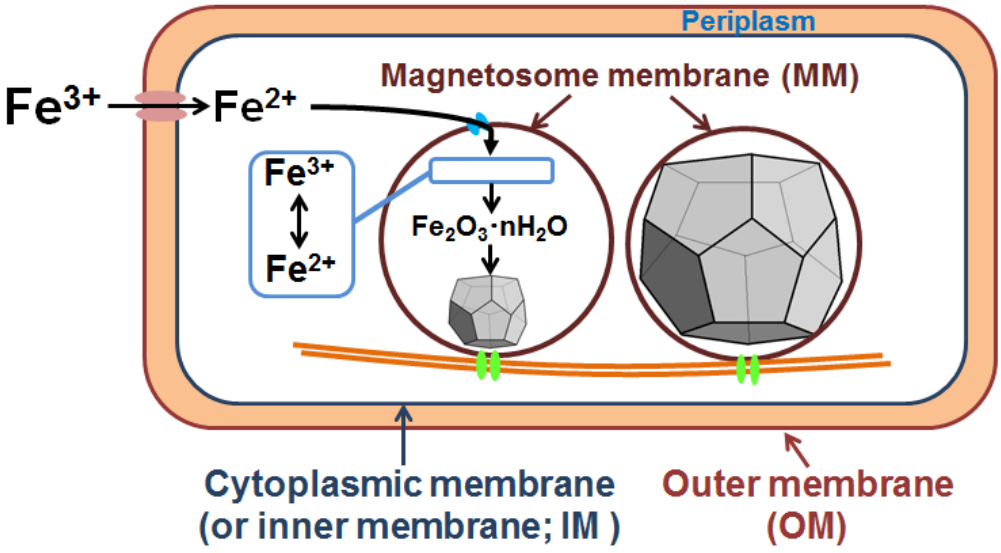

Fig. 6 Hypothetical model for magnetite biomineralization in *Magnetospirillum* species is provided by Schüler[17].

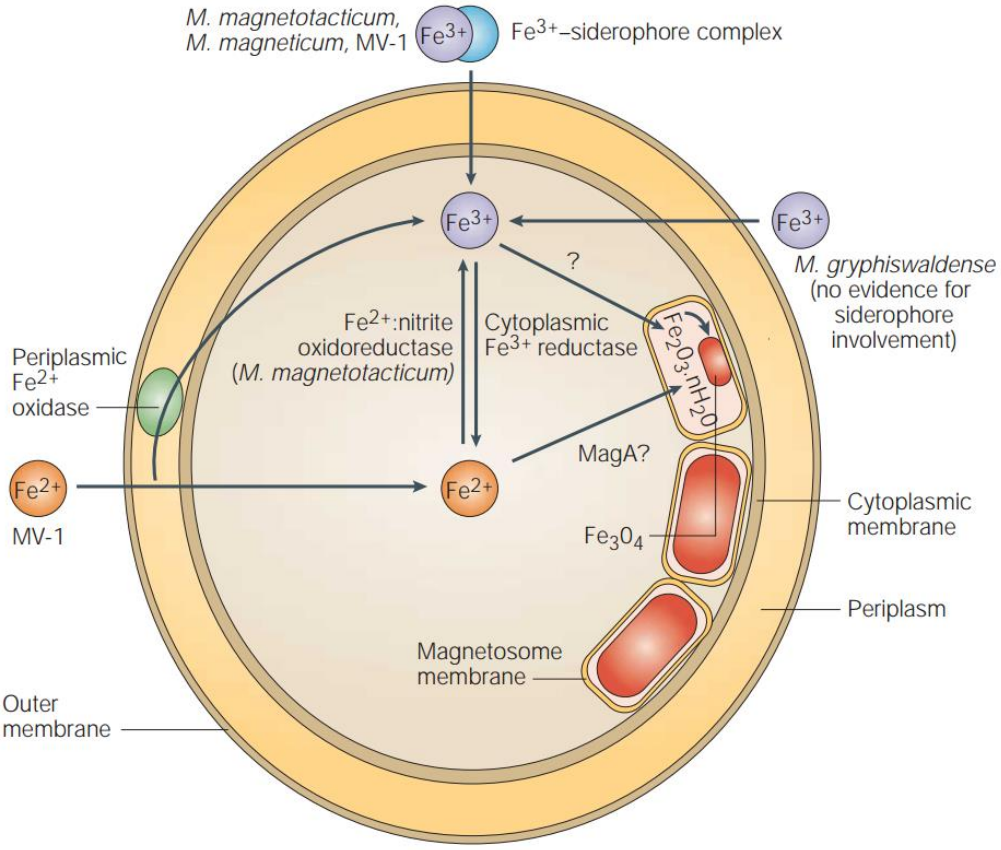

Fig. 7 Hypothetical model for magnetosome formation is provided by Bazylinski and Frankel[7].

1.2.3.1 Absorption of iron

Iron element usually exists trivalence (Fe^{3+}) in the natural. However Fe is insoluble in water in aerobic and neutral pH condition, so it cannot be directly absorbed by the cells. Therefore, many cells produce the low molecular weight of specific chelator which is combined with Fe^{3+} - “siderophore” which has a high affinity with Fe^{3+}[7, 44, 45]. Bacteria can absorb the iron chelator from insoluble iron source by using siderophore. Thus, siderophore has an important role for iron ions transport.

Paoletti and Blakemore[45] reported a role of hydroxamate type siderophore in uptake of iron by the cell at first. They indicated that MS-1 produced hydroxamate when cultured with high concentration (> 20 μM) of ferric quinate but not when grew with low concentration (5 μM). Galugay *et al*.[18, 46] reported the AMB-1 produced both hydroxamate and catechol siderophores by using the chrome azurol sulfonate assay and the ferrozine method. A concentration of at least 6 μM Fe^{3+} is required to initiate siderophore production. Bazylinski and Frankel[7] mentioned the MV-1 produced the hydroxamate type siderophore and the producing way was same as that of AMB-1. Dubbels *et al*.[47] indicated the siderophore production of MV-1 appeared to be repressed above and below initial iron concentration range of 8-28 μM, and they found the copper-dependent iron transport system in this strain. However, for the MSR-1 cell, no siderophore-like compounds could be detected in spent culture by using the

chrome azurol sulfonate assay[12, 42, 48].

1.2.3.2 Magnetite within magnetosome vesicle

Magnetite is surrounded by phospholipid bilayer *in vivo*, and which is called “magnetosome”. Therefore, the phospholipid bilayer - magnetosome vesicle effect on the magnetite crystal formation (Fig. 8 and 9).

Gorby *et al*.[6] presented the intact magnetosomes of MS-1 (*Aquaspirillum magnetotacticum* is written in original) were purified from broken cells by a magnetic separation technique and they provided the hollow magnetosome vesicle by electron microscopy (Fig. 8). They found, magnetosome vesicle was similar to the cytoplasmic membrane, which was both phospholipid bilayer and the contained amount of protein, and that was approximately 3-4 nm thick. Compositions of magnetosome vesicle mainly include free fatty acid, glycolipids, sulfide, phospholipids and other organic ingredient. The gel electrophoresis experiments showed the amount of protein of magnetosome vesicle can be detected in cytoplasmic membrane[6, 49]. Because of the similar composition of magnetosome vesicle and the cytoplasmic membrane, the magnetosome vesicle may be formed by the invagination and contraction of cytoplasmic membrane. Komeili *et al*.[50] observed the 3D ultrastructure of magnetosome by electron cryotomography (ECT) technique (Fig. 9). The hollow or contained part of the MNPs of magnetosome vesicle appeared *in vivo* when cells grew in lack iron growth medium. By this token, magnetosome vesicle is originated in the

cytoplasmic membrane.

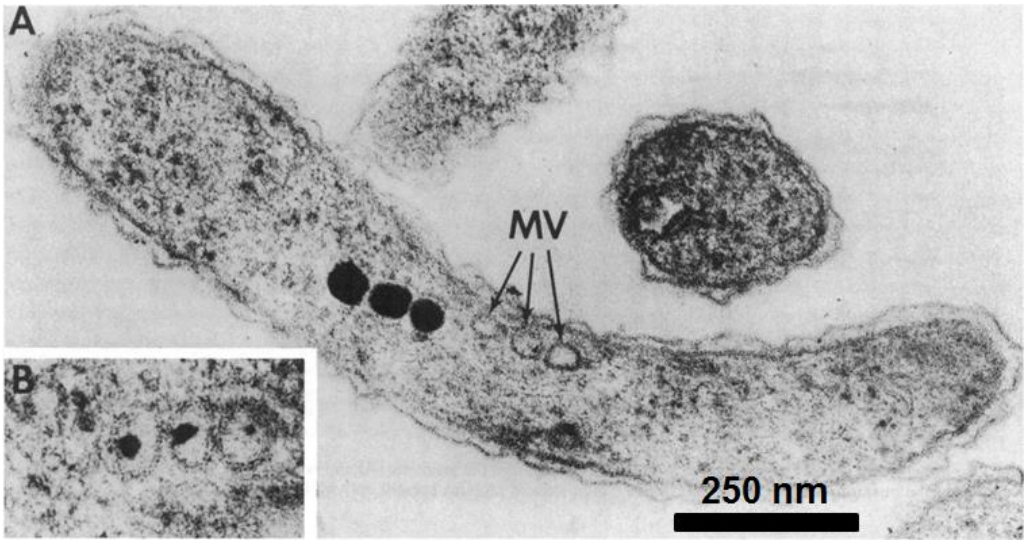

Fig. 8 Thin sections of *M. magnetotacticum* MS-1 are provided by Gorby *et al*.[6]. The arrows showed magnetosome vesicle (or membranous vesicle, MV) in Fig. A. The small electron-dense deposits of amorphous iron are represented in magnetosome vesicles (B).

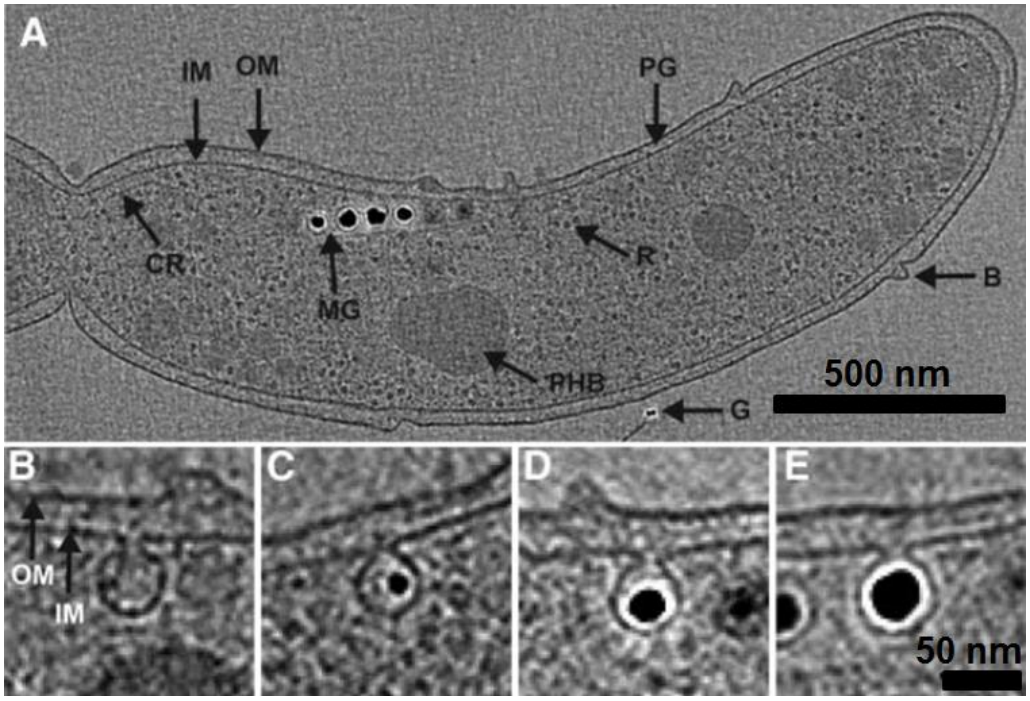

Fig. 9 *M. magneticum* AMB-1 membrane invagination formed magnetosome vesicle[50]. Figure (A) shows a 12-nm-thick section of an Electron cryotomography (ECT) reconstruction of AMB-1 cells. The process of magnetite crystal formed in magnetosome vesicle: no magnetite (B), small (C), medium (D) and fully-grown (E). (Outer membrane, OM; inner membrane, IM; peptidoglycan layer, PG; ribosomes, R; outer membrane bleb, B; chemoreceptor bundle, CR; poly-β-hydroxybutyrate granule, PHB; gold fiduciary marker, G; magnetosome chain, MG)

1.3 Magnetic properties of MTB

Inorganic MNPs are synthesized by MTB cells *in vivo*. They are arranged in chain structure in the cell, and particles are surrounded by lipid bilayer membrane (3-4 nm). They have narrow and uniform particle size (35-120 nm), and are highly pure of chemical composition (Fe_3O_4 or Fe_3S_4). These advantages give it unique magnetic properties. With the development of material science and biochemistry, new measurements techniques such as high-resolution transmission electron microscopy (HRTEM)[51], vibrating sample magnetometer (VSM)[52], superconducting quantum interference device (SQUID)[53-58], ferromagnetic resonance (FMR)[59, 60], magnetic force microscopy (MFM)[61], electron holography (EH)[62], Bacteriodrome[63] *etc*. are successfully applied to MTB cells, magnetosome or a chain of magnetosomes for testing the magnetic properties. They have greatly enhanced the magnetic information of magnetosome and promoted the applications of the magnetosome.

1.3.1 Magnetic properties of magnetosome MTB

Thomas-Keprta *et al*.[51] presented the according to the magnetite magnetosome in MTB analyzed by HRTEM as follows characteristics: (1) the single-domain size range with defined shape anisotropies and a narrow, asymmetric width-to-length (W/L) distribution; (2) magnetite crystals are chemically pure; (3) a unique crystal; (4) specific-crystal habit; (5) magnetite crystals are aligned in chain; (6) elongated along the zone axis. However, the TEM sample preparation was difficult; the observation process takes time and hard to quantitative analysis.

Moskowitz *et al*.[53-55, 57] investigated the magnetic properties and grain size of intact magnetosome of MTB by using SQUID. They summarized the characteristics of magnetic properties of magnetosome and MTB by comparison of temperature dependence of magnetization after zero-field cooling (ZFC) and field cooling (FC): (1) $R_{df} \approx 0.5$ (R denotes particle interaction; df is direct field demagnetization); (2) $R_{af} > 0.5$ (af is alternating field demagnetization); (3) ARM/SIRM = 0.15~0.25 (at $\mu_0 H_{applied}$ = 0.1 mT; ARM, anhysteretic remanent magnetization; SIRM, saturation isothermal remanent magnetization); (4) $\delta_{FC}/\delta_{ZFC} > 2$ ($\delta = (M_{80\ K} - M_{150\ K})/M_{150\ K}$; $M_{80\ K}$ and $M_{150\ K}$ are the remanence measured at 80 and 150 K, respectively). This is called “Moskowitz test”. Ratio of δ is deemed to identify bacterial magnetite; because of the magnetosome chain have significant magnetic anisotropy *in vivo* that gives higher δ_{FC}/δ_{ZFC} of the sample. The ratio of δ in MTB was 1.2-1.5. It may be the magnetosome suffered different levels damage[63-65]. Moskowitz test can be identified the MTB

contained the intact magnetosome chain, and ensured the purity of the magnetite in the sample[34, 55, 56, 66, 67]. However, this test unable to present the right judgments when the magnetite was oxidized or when the magnetosome is not arranged with a chain *in vivo*[55, 56, 59].

Verwey[68] found the artificially synthesized magnetite represented the phase transition at closely 120 K; the cubic structure distorted to the monoclinic structure when the temperature cooled to 120 K, which is called “Verwey transition” and “Verwey transition temperature (T_V)”. The other hand, the T_V value of MTB was approximately 100-110 K[55, 57, 59, 65, 67, 69], but some was different (MV-1[69]: 117 K; RS-1[70]: 88 K). According to this transition, Prozorov *et al*.[69] reported the T_V of various strains of MTB such as AMB-1 (102 K), MC-1 (102 K), MMS-1 (101 K) and MV-1 (117 K) using MPMS magnetometer. They referred that the T_V was not significantly affected in nanoparticles. Another magnetic signature of the Blocking temperature (T_B) was reported. They summarized the relationship between T_V and T_B in MTB as $T_V < T_B$, when the nanoparticles arranged in chains; conversely ($T_V > T_B$), the nanoparticles were not in chain structure.

The other characteristics of magnetic properties such as coercivity (H_c), remanence coercivity (H_r), saturation magnetization (M_s) and remanence magnetization (M_r) was reported[53-55, 65, 67, 69, 71, 72]. The value of H_c and M_s is different with different strain of MTB. The value of M_r/M_s ratio is approximately 0.45-0.5[55, 73], some is higher than this value[74].

1.3.2 Influence of the magnetosome arrangement on magnetic

properties

The magnetosome arrangement mode affects the magnetic properties of them, such as H_c, M_s, ratio of δ, value of T_V *etc*. Denham *et al*.[52] reported the magnetic properties of freeze dried magnetotactic bacterial cells (S-1), nonmagnetotactic bacterial cells (S-2), and extracted magnetosomes (S-3) from magnetotactic cells of MS-1 are measured by the VSM. The results showed that the value of H_c was decreased from 220 Oe (S-1) to 105 Oe (S-3) and the value of M_s (J_s is written in original) was increased 0.9 G-cm^2/gm (this unit is equal to emu/g) (S-1) to 13 G-cm^2/gm (S-3), and S-2 was nonmagnetic. The value of M_r/M_s (= J_r/J_s) was approximately 0.45 (S-1 and S-3 were 0.47 and 0.42, respectively). They obtained the magnetism of the individual cell resides in their magnetosome, however, the different magnetic properties between MTB cells and extracted magnetosomes is discussed unclear.

Moskowitz *et al*.[53] represented the magnetic properties of intact whole cells and magnetosome chain of MS-1 cells measured by SQUID magnetometer. The results indicated that the magnetic properties of magnetosome chain were different from that of the intact whole cells. It may be caused by the magnetostatic interactions[55]. Li *et al*.[71] reported about the comparison of magnetic properties between whole cells and isolated magnetosomes of AMB-1. The results showed the significant difference of magnetic properties among them. It was due to the spatial arrangement of magnetosomes and magnetostatic interaction. They presented the results of Moskowitz test: the ratio of δ within whole cells and isolated magnetosomes were 3.0 and 1.5,

respectively. The high δ-ratio of whole cells would result from was concluded as the result of the strong intrachain interactions and a weak interchain interaction generated by the non-interacting uniaxial single-magnetic domain particles. In the case of the isolated magnetosome, the magnetosome chains collapsed and magnetosome are closely packed without rules leaded to the increasing of the interchain interaction and interparticle interaction, which results in the reduced H_c and δ-ratio.

1.3.3 Chemical composition of magnetosome effect on their magnetic properties

The magnetic properties of magnetic substance are depend on their chemical composition, grain size, crystal defects, crystal orientation, and magnetic interaction *etc*. The range of crystal in magnetosome grain size is generally 35-120 nm long, which is a stable single magnetic domain, and the crystal grain size at both end of the magnetosome chain is smaller than common size (< 25 nm), that may have superparamagnetic (SPM)[70, 75, 76].

Recently, some researchers reported a few amount of transition metal elements are doped or incorporated into the magnetosome of the several strains of MTB. Staniland *et al*.[58] investigated Co doped into the magnetosome of model MTB (MS-1, AMB-1 and MSR-1) *in vivo* at first. That Co incorporated into the magnetosome when MTB were grown in the medium containing Co and that the size and H_c of magnetosome or intact cell increased, but the magnetic

signature of T_V (≈ 100 K) reduced. For analysis of Co element concentrations in each sample the X-ray absorption spectroscopy (XAS) and X-ray magnetic circular dichroism (XMCD), are used. They detected the Co merely near the surface of the magnetosome crystal but did not in the core of it. Kundu *et al*.[77] reported about the change in bacterial size and magnetosome features for MS-1 cultured under high concentrations of zinc (Zn) or nickel (Ni). The size of magnetosomes of the bacteria cultured in the presence of Zn or Ni (mean size was 23 and 25 nm) is considerably larger than that of magnetosomes in the control set (Fe; mean size was 15 nm). The magnetization per cells of MS-1 grown in Zn or Ni culture was significantly higher than that of the control. H_c value was almost the same for Zn containing and normal MS-1, and that of the decreased with Ni is presented in the medium. Energy Dispersive X-ray (EDAX) detected the presence of Zn in or associated with the magnetosomes. The atomic percentage (at.%) of Fe and Zn were 61.34% and 21.88% respectively, but Ni was not detected. It is worth mentioning that the grain size of magnetosomes was smaller than the common[78], which might be due to cultured conditions. The change of magnetic properties in each sample was not discussed in detail.

Recently, Tanaka *et al*.[79] reported the highest doping of transition metal element (*e.g.*: Mn^{2+}: 2.7%, Co^{2+}: 3.0%, and Cu^{2+}: 15.6%) into magnetosomes *in vivo* when MTB strain AMB-1 were grown in the medium containing Mn, Co, Cu, Zn or Ni. However, Zn and Ni element were not detected in this studied. Increased concentrations of metal, except for Mn, retarded cells growth and magnetite crystals formation. But, they were not significantly difference in low

concentrations of Ni and Zn (< 20 μM) conditions. In this case, we can preliminary deemed that the absorption of transition metal was likely to be different or have different choice with different strains of MTB. Variable-temperature magnetization curves data were provided the T_V at lower temperature (Mn: $T_{V\text{-}Mn}$ = 92 K; Cu: $T_{V\text{-}Cu}$ = 96 K) to the control samples (Fe: $T_{V\text{-}control}$ = 106 K). In addition, H_c value that doping of Mn or Cu reduced (Mn and Cu: 0.08 T) compared with control sample (Fe: 0.11 T) at low-temperature (10 K), but not obviously different at high-temperature (200 K). As similar report, the observing only Mn (1.0-1.1%) in magnetosomes of MSR-1 grown in medium containing 50 μM of Mn, ruthenium (Ru), vanadium (V) and Zn that was reported by Prozorov *et al*.[80] last year. In morphology or in size of magnetosome magnetite crystals did not show any significant difference that the cells grew in the presence or not a doping metal medium. They demonstrated that the magnetic properties especially T_V of magnetite of MTB can be significantly affected by the incorporation of metal ions such as Mn.

1.4 Purpose of the present study

Although the ferric iron (Fe^{3+}) concentrations affects the magnetosome formation has been reported, however, the Fe^{3+} concentrations affect the magnetic properties of magnetosome MTB are limited, usually at 25 or 34 μM Fe^{3+}. In Chapter 3 part 1 of my thesis, the influence of ferric (Fe^{3+}) iron on the magnetic properties of *M*. *magnetotactic* MS-1 was described. The purpose of this part of

the thesis is to clarify the effect of the initial Fe^{3+} concentration on the yield and magnetic properties of the magnetosomes formed by *M*. *magnetotactic* MS-1.

“Pure” and narrow size distribution of magnetite is produced by MTB *in vivo*. However, application of MTB is confined these: 1) unitary larger grain size (average approximately 50 nm); 2) narrow range of magnetic properties. Hence, the changed or innovated characteristics of magnetite magnetosome that improve or broaden the application of them. This biomineralization process is highly regulated by the cell, rendering the crystals highly chemically pure. Recently, doping of transition metal into the MTB resulted in the characteristics of them is altered. However, they discussed only intact cell level. What took place in magnetite magnetosome level *in vivo*? I presented the magnetic properties of MTB grew in growth medium with standard, Zn-doping or Co-doping in the Chapter 3 part 2 of my thesis. The purpose of this part is to investigate the influence of Zn or Co element on the magnetosome or magnetite in MTB.

Chapter 2 Materials and Methods

In this study, we used the model MTB strain MS-1 which grew in different conditions and separated the different samples such as intact cell, magnetosome and magnetite (Section 2.1). The grain size, magnetic properties and the element of the MS-1 cells were measured by the transmission electron microscope (TEM), magnetic property measurement system (MPMS) and electron probe microanalysis (EPMA), respectively.

2.1 Preparation of sample

Intact cell, magnetosome and magnetite sample is focused on our study. The details of samples and methods are shown as following section.

2.1.1 Bacterial strain and cultural conditions

The magnetotactic bacterium strain *Magnetospirillum magnetotacticum* MS-1 (ATCC31632) was used to grow in standard Magnetic Spirillum Growth Medium (MSGM, Table 1). The composition of the standard MSGM contain with basically solution, Wolfe's (mineral and vitamin) solution (Table 2 and 3), and 0.01 M ferric quinate (as showed in Table 4). The pH of all culture media was set to 6.75 by addition of 10 N NaOH. They were autoclaved for 20 min at 121 ºC.

The Wolfe's vitamin solution with 0.002 g/L of L(+)-Ascorbic acid sodium salt was appended to the MSGM medium by using 0.45 μM filter (MILLEX-HA, Japan) before the implanted cells. For the concentration of O_2 kept below the 2% (microaerobic condition), the MSGM medium was added in a screw-capped glass bottle at the top of the bottleneck. The cells grew at 26 °C in present work.

Table 1 The components of MSGM medium

Wolfe's Vitamin solution	10.0	mL
Wolfe's Mineral solution	5.0	mL
0.01 M Ferric quinate	2.0	mL
Resazurin	0.45	mL
KH_2PO_4	0.68	g
$NaNO_3$	0.12	g
Ascorbic acid	0.035	g
Tartaric acid	0.37	g
Sodium acetate	0.05	g
Distilled water	1.0	L

Table 2 Wolfe's Mineral solution

Nitrilotriacetic acid	1.5	g
$MgSO_4 \cdot 7H_2O$	3.0	g
$MnSO_4 \cdot H_2O$	0.5	g
NaCl	1.0	g
$FeSO_4 \cdot 7H_2O$	0.1	g
$CoCl_2 \cdot 6H_2O$	0.1	g
$CaCl_2$	0.1	g

$ZnSO_4 \cdot 7H_2O$	0.1	g
$CuSO_4 \cdot 5H_2O$	0.01	g
$AlK(SO_4)_2 \cdot 12H_2O$	0.01	g
H_3BO_3	0.01	g
$Na_2MoO_4 \cdot 2H_2O$	0.01	g
Distilled water	1.0	L

Table 3 Wolfe's Vitamin solution

Biotin	2.0	mg
Folic acid	2.0	mg
Pyridoxine HCl	10.0	mg
Thiamine HCl	5.0	mg
Riboflavin	5.0	mg
Nicotinic acid	5.0	mg
Calcium (+)-pantothenate	5.0	mg
Vitamin B_{12}	0.1	mg
p-Aminobenzoic acid	5.0	mg
Thioctic acid	5.0	mg
Distilled water	1.0	L

Table 4 0.01 M Ferric quinate (Fe-quinate)

$FeCl_3$	0.27	g
Quinic acid	0.19	g
Distilled water	100.0	mL
Dissolve and autoclave at 121 °C for 5 minutes.		

2.1.1.1 Culture condition with different ferric iron concentration

We cultured MS-1 cells in MSGM under microaerobic conditions at 26 °C for one week in screw-capped glass bottles (500 mL), as previously described[81]. The Fe^{3+} concentration of the standard MSGM medium is usually 34 μM. It was modified to 0 μM, 12 μM, 22 μM, 34 μM, and 68 μM. Hereafter, these concentrations are referred to as GM(0), GM(12), GM(22), GM(34), and GM(68). Under all culture conditions, Fe^{2+} was added to the GM as $FeSO_4 \cdot H_2O$ to produce a final concentration of 3.8 μM.

2.1.1.2 Transition metal in culture medium

MS-1 cells were grown in a screw-capped glass bottles (5 L) under microaerobic conditions for one week at 26 °C as previously described[58, 72, 77, 81]. In this section, the transition metal of Zn or Co in MSGM medium was modified by zinc quinate (Zn-quinate; Table 5) or cobalt quinate (Co-quinate; Table 6). The total metal concentration was finally fixed at 34 μM as shown in Table 7.

Table 5 Zinc quinate (Zn-quinate)

$ZnCl_2$	0.23	g
Quinic acid	0.19	g
Distilled water	100.0	mL

Table 6 Cobalt quinate (Co-quinate)

$CoCl_2 \cdot 6H_2O$	0.40	g
Quinic acid	0.19	g
Distilled water	100.0	mL

Table 7 The ratio of Fe-, Zn- and Co-quinate in growth medium

Contents (μM)	Fe	Fe/Zn	Fe/Co
Fe-quinate	34	22	22
Zn-quinate	0	12	0
Co-quinate	0	0	12

2.1.2 Separation of intact cell, magnetosome and magnetite

The analyzing samples such as intact cell (IC), magnetosome (MG) and magnetite (MT) were isolated from the growth medium as following steps.

The cultured cells were harvested by centrifugation at 6,000 ×g for 20 min at 4°C (Kubota 7780, Kubota, Osaka, Japan) and/or at 12,000 ×g for 10 min at 4°C (Kubota 6200, Kubota, Osaka, Japan). The precipitation cells were then washed five times by centrifugation and resuspended in 1 mL of 50 mM Tris-HCl buffer (pH 6.8). The suspension was placed on the magnet (TOYOBO Magical Trapper MGS-101) for overnight at 4°C. Cells containing magnetosome, magnetic cells were captured on the tube wall on the magnetic side. The separation with the magnet was repeated five times to obtain only magnetic cells, which was named “intact cell (IC)” sample. This step was repeated five times. The cells not

captured by magnet and remained in the media were collected by centrifugation as a non-magnetic cell.

The separation and purification of the magnetosomes and magnetite: the magnetic cells were suspended in 50 mM Tris-HCl (pH 6.8), and disrupted by ultrasonic homogenizer with 20 kHz at 70 W (amplitude 30%) for a total period of 5 min and centrifuged at 10,000 ×g for 5 min at 4 ºC to check the amount of the precipitate, unbroken cells. To fully disrupt the cells, we usually repeated the sonication for five times. After the cells were fully disrupted, the extract was placed on the magnet for one hour. Magnetosomes were captured at the magnet sidewall of the tube, and that was called “magnetosome (MG)” sample. For the purified magnetosome, the samples were washed by 50 mM Tris-HCl (pH 6.8) buffer and were separated with magnet; this step was repeated five times. The purified magnetosomes were removed to the 1.5 mL tube, and resuspended in 10 N NaOH at 95 ºC for 15 min, then centrifuged at 1,000 ×g for 10 min at 4 ºC, after that the precipitation was suspended in 1 mL 50 mM Tris-HCl and the magnet separated magnetite from the washing buffer (pH6.8 of 50 mM Tris-HCl) for one hour. In order to obtain high purity magnetite, this step was repeated five times. The purified magnetite was called “magnetite (MT)” sample.

The each sample was dried by vacuum centrifugal concentrator (VC-36N, TAITEC, Saitama, Japan), and dried samples were wrapped in aluminum paper for magnetic measurements.

2.2 Characterization of MS-1 cells

For the biological characterization of cells, we analyzed the cells growth by using UV-visible spectrophotometry; and the iron concentration in the growth medium was determined by using the 1,10-phenanthroline method, as described previously[82-84]. The cells production was measured by using an electronic balance. The characterization of grain size, magnetic properties and element analysis of MS-1 cells measured by using the transmission electron microscope (TEM), magnetic property measurement system (MPMS) and electron probe microanalysis (EPMA), respectively.

2.2.1 Growth curve and cells yield analysis

The cells growth was measured by using the UV-visible spectrophotometry (UVmini-1240, Shimadzu, Kyoto, Japan). Two mL of sample which was containing cells and growth medium was removed to the two 1.5 mL tube (1 mL sample per one tube). For the keeping the total volume of growth medium, we added the spare MSGM medium (without Fe element) into the growth medium at the same volume of the removing sample. One mL sample was measured the absorbance at 600 nm directly, and this measuring result was called “total cells growth”. The other tube was placed on the magnet for one hour and the magnetic cells were captured at the magnetic sidewall of the tube, whereas residual cellular materials (non-magnetic cells) were retained in the tube. The supernatant sample was removed to a new tube and was measured the

absorbance at 600 nm. And which was called “non-magnetic cells growth”. The difference between intact cells and non-magnetic cells growth were “magnetic cells growth”.

The weight of the precipitated IC, MG and MT was measured by using an electronic balance (readability: 0.1 mg; Sartorius CP64, Sartorius, Gottingen, Germany).

2.2.2 1,10-phenanthroline method

Generally, MTB growth in the MSGM growth medium which contains the micromolar levels of iron ions. And that, the ferrous (Fe^{2+}) and ferric (Fe^{3+}) iron in parallel exist in medium, therefore, the determination of concentrations of them is difficult. The ortho-phenanthroline (1,10-phenanthroline; Phen) is an organic reagent which is reacted with Fe^{2+} ions and forms a red color of 1,10-phenanthroline iron(II) complex ($(Phen)_3Fe^{2+}$) (Eq. 1). The iron ions in the growth medium analyzed by using 1,10-phenanthroline method[82-84].

$$Fe^{2+} + 3\ Phen \rightarrow (Phen)_3Fe^{2+} \qquad \text{(Eq. 1)}$$

The complexity of $(Phen)_3Fe^{2+}$ can appear in the peak at 510 nm by using UV-visible spectrophotometry. Therefore, the measuring sample was prepared as following: the sample centrifuged 10,000 ×g for 5 min at 4 ºC and the supernatant which contained Fe^{2+} and Fe^{3+} ions are removed to a new tube at stationary phase. The 500 µL of sample was reacted with each reagent solution as Table 8. All of Fe^{3+} ions are reduced to Fe^{2+} ions via strong reducing reagent

10% hydroxylamine hydrochloride (1 g $NH_2OH{\cdot}HCl$ in 10 mL of dH_2O). However, in order to distinguish between Fe^{3+} and Fe^{2+} in the same medium, one was added with $NH_2OH{\cdot}HCl$ (Total-Fe^{2+} sample), the other was without (Fe^{2+} sample). The difference between both them was concentration of Fe^{3+}. The reaction of the Phen is optimal under the weak acidity (pH ≈ 5.5) condition which controls with the buffer solution (6.80 g of CH_3COONa in 50 mL of dH_2O and the pH set to 4.6 by CH_3COOH, and the final volume to 100 mL). 5.5 mM of Phen (0.036 g Phen in 100 mL of dH_2O) add in the above solution and the total volume is 1 mL, and it stands at room-temperature for 30 min before the measurement.

Standard curve is prepared in accordance with table 9 and standard Fe^{2+} solution is made by ferrous ammonium sulfate ($FeSO_4(NH_4)_2{\cdot}6H_2O$). The concentration of 1.0 mg/mL Fe^{2+} was produced by 3.51 g $FeSO_4(NH_4)_2{\cdot}6H_2O$ in 500 mL of dH_2O, and add 12M HCl in it to keep the concentration of Fe^{2+} in the medium. Each sample was evaluated three times. In order to eliminate the interference of growth medium, the measurement standard curves parallel add with the 500 mL of standard growth medium without Fe ions (Table 9).

Table 8 Reagents for analyzing Fe^{2+} and total-Fe^{2+} (Fe^{2+}+Fe^{3+}) in medium

Reagents (μL)	Fe^{2+}	Total-Fe^{2+}
Sample	500	500
$NH_2OH{\cdot}HCl$	0	30
CH_3COONa	70	70
Phen.	70	70
dH_2O	360	330
Total	1000	1000

Table 9 Standard curve of S-Fe^{2+} (S means standard)

Con. of S-Fe^{2+} (μM)	S-Fe^{2+} (μL)	S-medium (μL)	dH_2O (μL)
0	0	500	330
2.5	14	500	316
5	28	500	302
10	56	500	274
20	112	500	218
40	224	500	106

2.2.3 Transmission electron microscope (TEM) analysis

One milliliter of the cells were transferred to plastic tube (1.5 mL), and harvested from the growth medium by centrifuged the culture at 6,000 ×g for 20 min at 4 ºC. The pellet samples were suspended and washed by five times in 50 mM Tris-HCl (pH 6.8) buffer. The pure cells were resuspended in same buffer and separated by using magnetically on magnet for 2 hours. In order to obtain pure magnetic cells, this step is repeated 3-5 times. The purified magnetic cells were resuspended in 10 mM Tris-HCl (pH 6.8) buffer; and then, the 5 μL samples were spotted onto 200-mesh copper grids and dried at room-temperature overnight. Dried samples were analyzed by using transmission electron microscope (TEM, 4000FX, JEOL, Japan, Fig. 11a) analysis working at acceleration voltage of 200 kV. Approximately 10 cells were chosen for this study. The size of magnetosome was determined by using the FV10-ASW software of

the best-fitting of the bright-field TEM images. Length (L) and width (W) of the magnetosomes was defined: a direction along magnetosome chain axis was L, and perpendicular to magnetosome chain axis was W (Fig.11b). The grain size was defined as (L+W)/2, and the shape factor (*k*) was described the elongation of the crystals, and defined as W/L[65]. The significance of differences in grain size and shape factor was analyzed by using Student's t-test. Significance was set to $p < 0.01$.

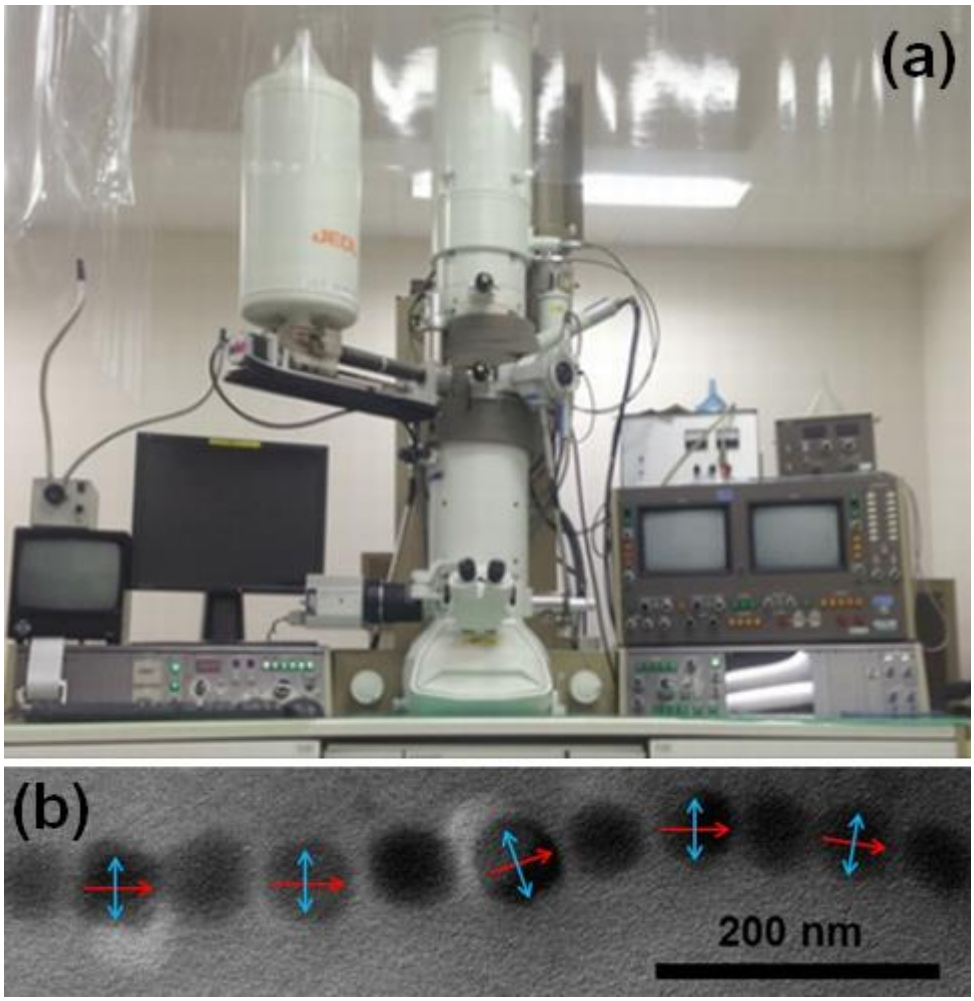

Fig. 11 Image of the transmission electron microscope (TEM) from the homepage of the Center for Instrumental Analysis of Muroran Institute of Technology. (a). The length (L; red arrow) and width (W; blue arrow) of a

magnetosome was defined (b).

2.2.4 Analysis of magnetic properties with MPMS

The magnetic properties of sample were analyzed by using magnetic property measurement system (MPMS, Ever Cool MPMS-2, Quantum Design, San Diego, USA) which sensitivity was 1.0×10^{-8} emu (Fig. 12). The hysteresis loop was measured between -10^4 and 10^4 Oe at room (300 K) or low (10 K) temperature, and the magnetic parameters of the samples, such as coercivity (H_c), saturation magnetization (M_s), and saturation remanence (M_r), were determined. Variable temperature magnetization data, both zero-field-cooled (ZFC) and field-cooled (FC), were measured as follows: 1) the temperature was cooled from 300 K to 10 K in zero magnetic field and data were obtained while the sample was warmed from 10 K to 300 K at 1000 Oe; 2) FC data were obtained during cooling from 300 K to 10 K under the same field. The Verwey transition temperature (T_V) was determined according to the method described in Tanaka *et al*.[79] and the temperature at the maximum of the ZFC curve was read as the blocking temperature (T_B)[85]. Magnetic data were analyzed and plotted using OriginPro 8.0 software.

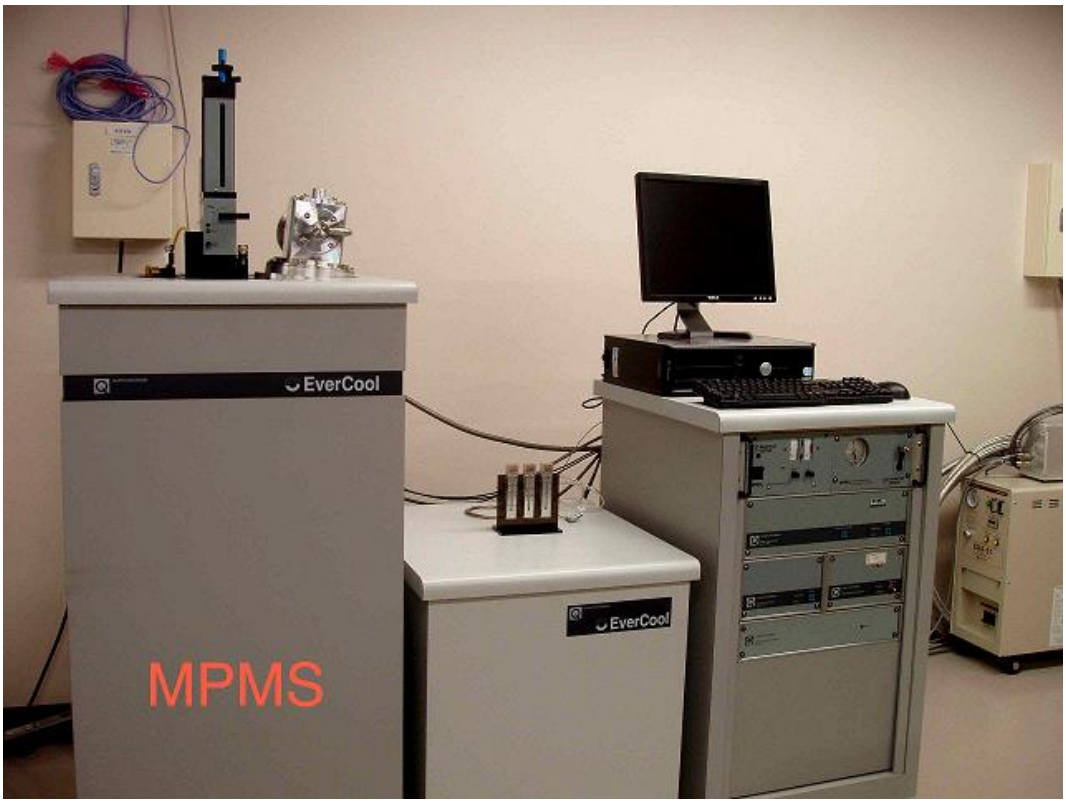

Fig. 12 Image of the magnetic property measurement system (MPMS) from the homepage of the Center for Instrumental Analysis of Muroran Institute of Technology.

2.2.5 Analysis of metal element with EPMA

The metal element was analyzed by using electron probe microanalyzer (EPMA, JXA-8900R, JOEL, Japan) in this study (Fig. 13a). The EPMA sample was prepared as following: firstly, the good electrical conductivity of double sided conductive (DSC) carbon tape was posted on the copper sample holder, and then the completely dried magnetosomes or magnetite sample were fixed onto a DSC-carbon tape layer. For the DSC-carbon tape support deposition of the

magnetosomes or magnetite was used by using vacuum evaporator (JEE-400, JOEL, Japan) for 30 min at room-temperature. The magnetosome was formed by Fe_3O_4 was packaged with phospholipid. So, in order to increase the electrical conductivity, a conductive layer, like carbon or gold, must be spread on the surface of magnetosomes. Choice gold was used with conductive layer and magnetosomes or magnetite was used by ion sputter (JFC-1100, JOEL, Japan) for gold-plated. The cemented magnetosomes or magnetite were plated with gold at operating voltage of 1.2 kV and a working current of 5.0 mA under low vacuum for 1.5 min. The final gold thickness was approximately 5-7 nm. And last, the completely gold-plated magnetosomes or magnetite were fixed on the sample stage with DSC-carbon tape prior to analysis (Fig. 13b). The operating voltage was 15.0 kV and a working current was approximately 2.0×10^8 A. The metal element (M) concentration was calculated by the equation: M/(Fe+M) × 100 (%) (M = Zn or Co).

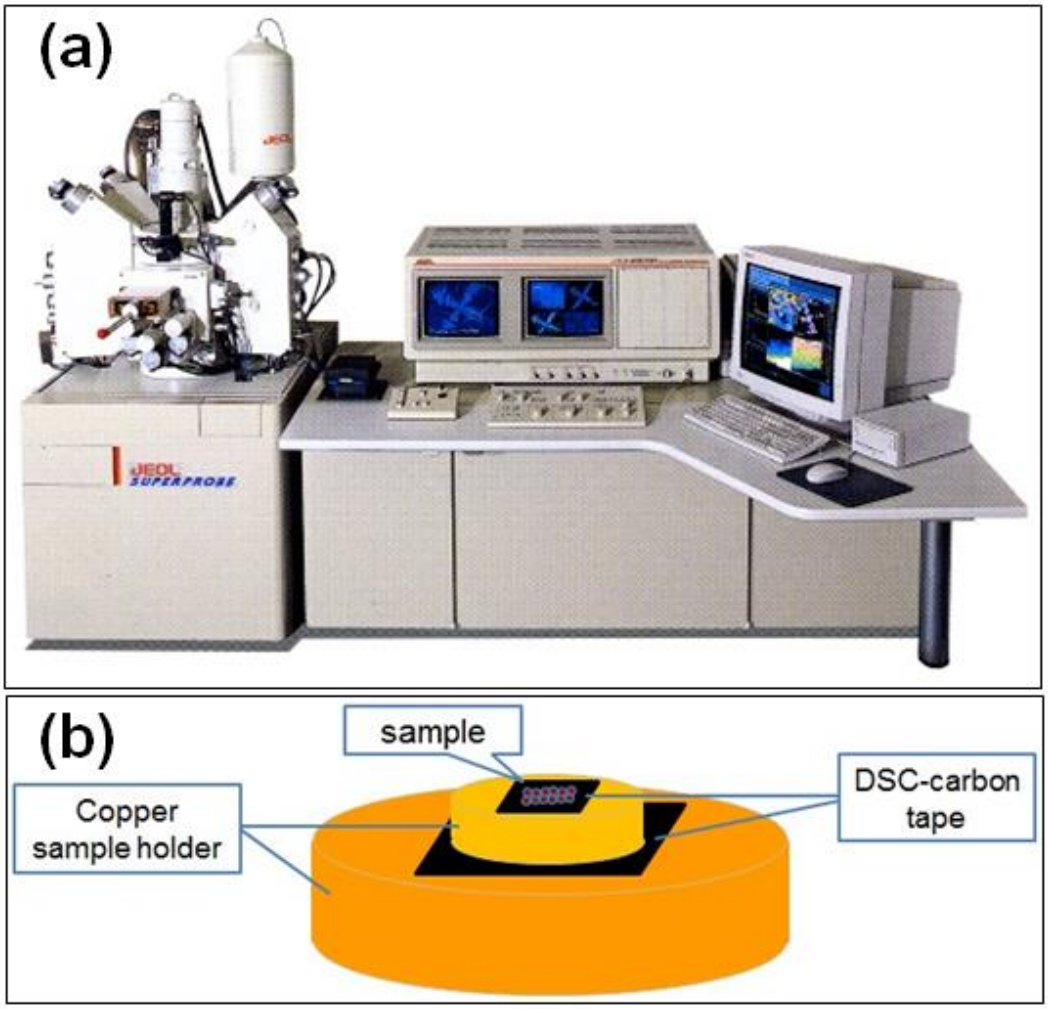

Fig. 13 JXA-8900R-type electron probe microanalyzer (EPMA; photo from the homepage of the Center for Instrumental Analysis of Muroran Institute of Technology) (a) and preparation of EPMA sample (b).

Chapter 3 Results and Discussions

3.1 Magnetic properties of magnetite synthesized by *Magnetospirillum magnetotacticum* MS-1 cultured with different concentrations of ferric iron

Biomineralization and formation of magnetite by MTB begin with uptake of iron from the external medium. Thus, the concentration of ferric iron (Fe^{3+}) in the culture medium affects the process. Noguchi *et al*.[86] reported that the average number of magnetosomes per cell decreased in parallel with the Fe^{3+} reductase activity of the soluble fraction when cells were cultivated in medium containing less than 5 μM Fe^{3+} quinate. The total cell yield, however, was not affected by low Fe^{3+} concentrations. Although the effect of Fe^{3+} concentration on the yield of cells and magnetosomes has been investigated[86], few studies have investigated how the Fe^{3+} concentration affects the magnetic properties of the magnetosome, and the magnetic properties of MTB strain MS-1 have only been investigated at 25 or 34 μM Fe^{3+} [52, 53, 55].

The present work in this part aimed to clarify the effect of the initial Fe^{3+} concentration on the yield and magnetic properties of the magnetosomes formed by *M. magnetotacticum* MS-1. We analyzed the yields of magnetic and nonmagnetic cells and magnetization in relation to the magnetic field strength and temperature using a MPMS.

3.1.1 Yields of cells

Yields of total and magnetic cells MS-1 cells grew and formed magnetosomes

in media containing different Fe^{3+} concentrations. The yields of MS-1 cells at different Fe^{3+} concentrations are shown in Fig. 14. The total cell weight was not dependent on the initial Fe^{3+} concentration; yields were 0.12-0.15 g/L of culture, which were smaller than the yield of 0.2-0.5 g/L reported by Blakemore *et al*.[8] and Noguchi *et al*.[86]. Although the reason for the difference in total yield is not clear, the result that the initial Fe^{3+} concentration did not affect total cell yield was consistent with a previous study by Noguchi *et al*.[86].

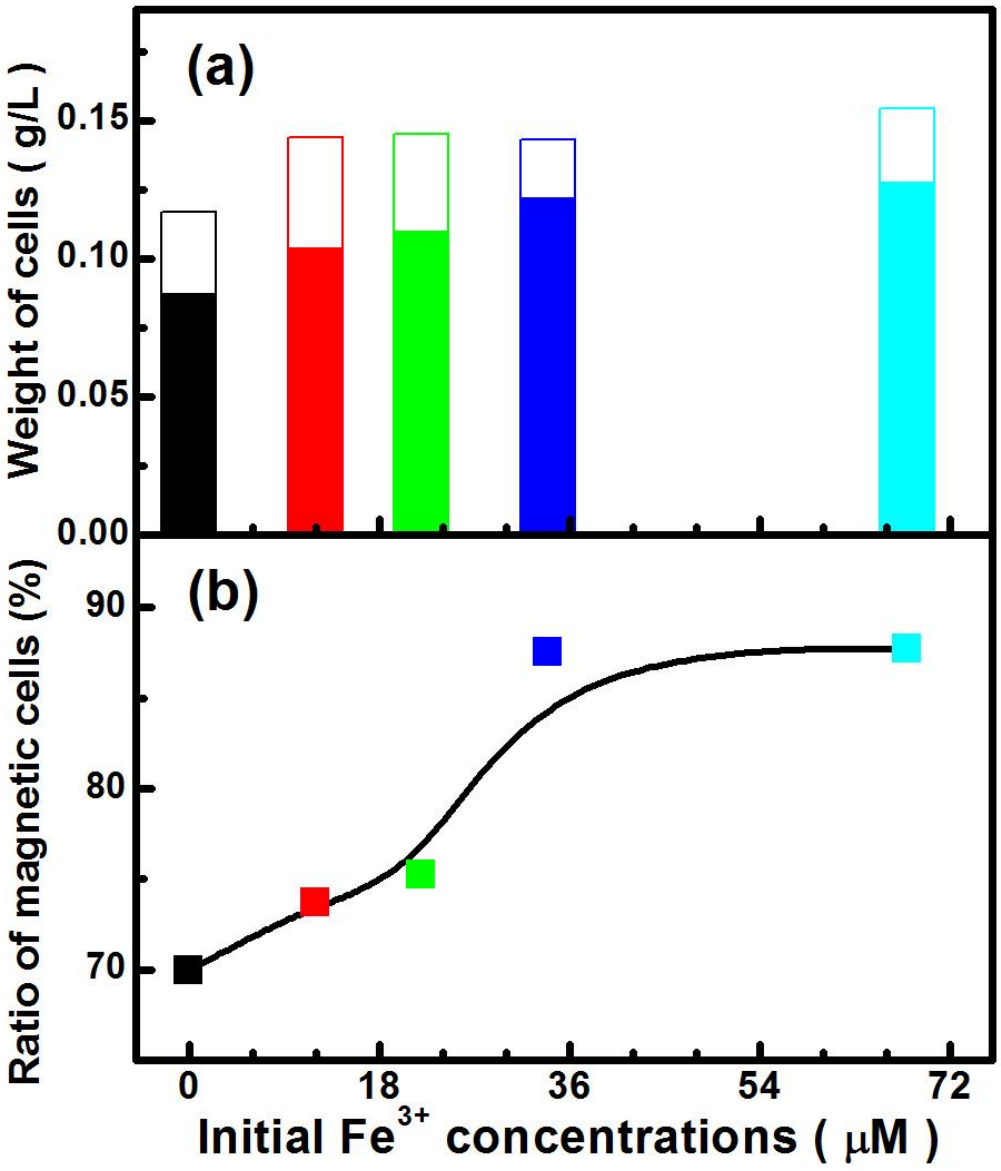

Fig. 14 The total weight *M. magnetotacticum* MS-1 cells grown at various initial concentrations of Fe^{3+}. (a) The weight per liter of culture of magnetic (solid bars) and nonmagnetic (open bars) cells. (b) The ratio of magnetic

cells to total cells (weight of magnetic cells/weight of total cells × 100).

We separated magnetic cells (solid bars) from nonmagnetic cells (open bars). The yields are shown in Fig. 14a. The weight of magnetic cells increased as the initial Fe^{3+} concentration increased. Nearly 70% of the total cells were magnetic even in GM(0); this increased to nearly 90% in GM(34) and GM(68) (Fig. 14b). Thus, the quantity of magnetosomes increased when MS-1 cells were grown at higher Fe^{3+} concentrations.

The final concentrations of Fe^{2+} and Fe^{3+} in the GM were measured and compared with the initial values. As shown in Fig. 15, the concentration of Fe^{3+} greatly decreased in GM(12)-GM(68), whereas the concentration of Fe^{2+} changed only slightly after culture. Iron uptake by MS-1 cells ranged from 1.5-46 μM, depending on the initial iron concentration.

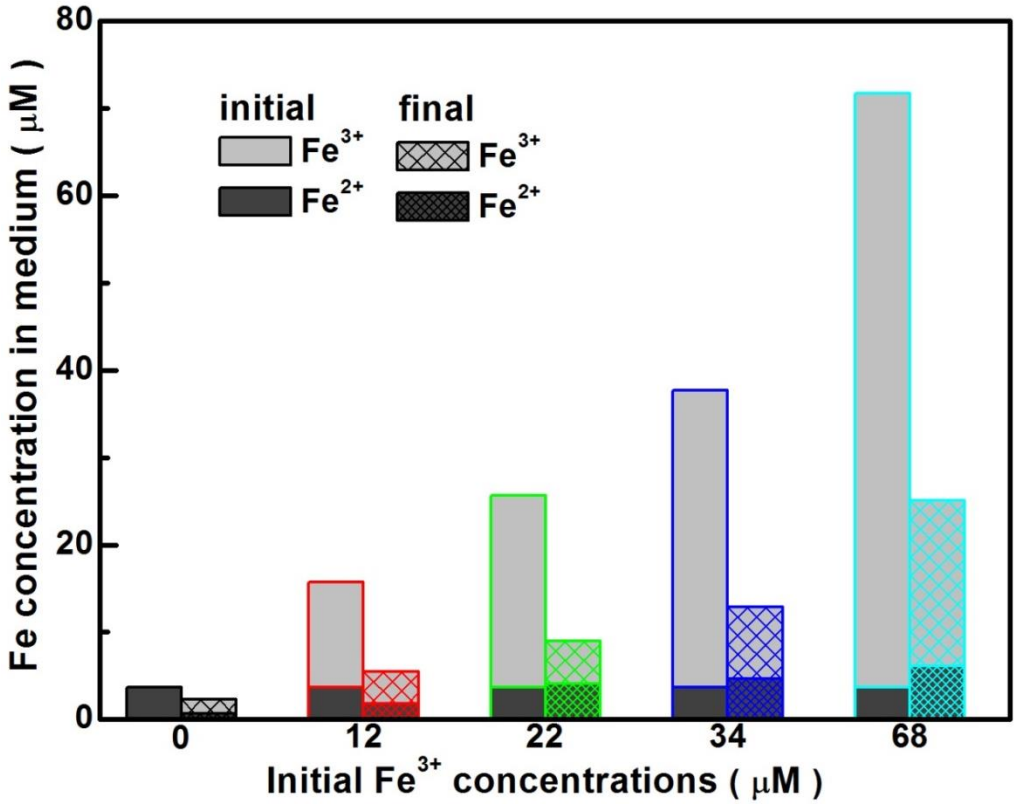

Fig. 15 Initial and final iron concentrations in the growth medium (GM). The

"initial" represents the calculated concentrations of Fe^{2+} and Fe^{3+} added to the GM. The "final" represents the concentrations of Fe^{2+} and Fe^{3+} measured in the GM following culture.

3.1.2 Magnetic properties of cells

The hysteresis loops of MS-1 cells grown at different initial Fe^{3+} concentrations were measured at 20 °C; two are shown in Fig. 16. The saturation hysteresis loops showed thick waists at low field strengths (<1000 Oe) and closed at 600 Oe (Fig. 16a and b). Magnetization of MS-1 cells saturated at approximately 2000 Oe (Fig. 16c). All cells cultured in all GM, GM(0)-GM(68), showed near-classic Stoner-Wohlfarth hysteresis loops, as reported by Moskowitz *et al*.[53].

The H_c value of cells cultured in GM(0) was 203 Oe; this value increased to 238 Oe when cells were cultured in GM(34) (Fig. 17a and Table 10). The H_c value depends on magnetic particle characteristics such as grain size, crystal defects, and/or magnetic interactions *in vivo* [65, 87]. The magnetite grain size of MS-1 cells varied from 30 - 70 nm, and the average grain size was *ca*. 50 nm (our unpublished data). The Hc value of chemically synthesized Fe3O4 particles (grain size; 50 nm) was reported to be 156-175 Oe[88, 89]. The H_c value of MS-1 cells was larger than that of chemically synthesized Fe_3O_4 and was reported to be 220 Oe (star[52] in Fig. 17a) or 268 Oe (pentagon[53] in Fig. 17a) at 25 μM Fe^{3+} (Table 10). The H_c value of MS-1 cells reached its maximum in cells grown in GM(34), and was slightly lower at a higher initial Fe^{3+} concentration, GM(68). One possible explanation for the low H_c value of cells grown at a lower initial Fe^{3+} concentration is that these cells may have a shorter magnetosome chain than that observed in cells grown at higher Fe^{3+}. Alternatively, magnetite particles may be smaller at low Fe^{3+} concentrations.

The M_s value of cells grown in GM(0) was 0.56 emu/g and that of cells

grown in GM(34) was 0.96 emu/g (Fig. 17 and Table 10). The M_s value of MS-1 cells cultured at 25 μM Fe^{3+} was reported to be 0.6 (shown as pentagons[53] in Fig.17b) or 0.9 emu/g (shown as stars[52] in Fig. 17b). The M_s value reported here (GM(22)) is consistent with that in a previous report by Denham *et al*.[52]. The M_s value of MS-1 cells grown in GM(0) was smaller than the others. The M_s value is determined by the chemical composition of the magnetic particles and is related to crystal defects and crystal orientation[53]. One possible explanation for the small M_s value of cells grown in GM(0) is that the magnetite crystals may be composed of other forms of iron oxide, such as maghemite (γ-Fe2O3). Other possibilities, such as crystal defects, cannot be excluded as factors that influence the magnetic properties of MS-1 cells grown in GM(0).

Table 10 Summary of magnetic properties of MS-1 cells grown at various initial concentrations of Fe3+ (-: not reported)

Fe^{3+} *Conc.* (μM)	0	12	22	34	68	25[52]	25[53]	34[55]
H_c (Oe)	203	216	230	238	230	220	268	-
M_s (emu/g)	0.56	0.84	0.90	0.96	0.85	0.9	0.6	-
M_r/M_s	0.49	0.52	0.50	0.51	0.53	0.47	0. 53	0.43
T_V (K)	88	97	97	95	96	-	-	100
T_B (K)	150	125	120	110	110	-	-	-

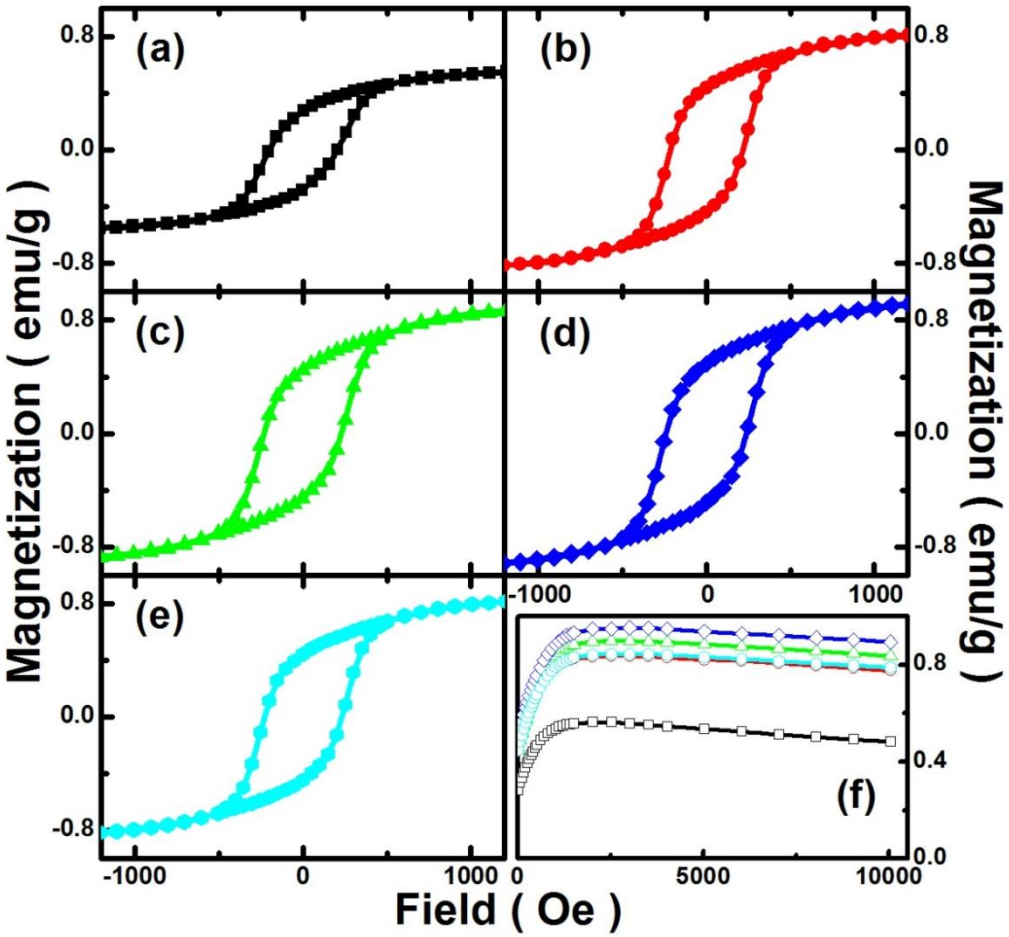

Fig. 16 The hysteresis loops of *M. magnetotacticum* MS-1 cells grown in GM (0) (a), GM (12) (b), GM (22) (c), GM (34) (d), and GM (68) (e) between -1300 Oe and 1300 Oe. The M_s of cells grow in GM (0) (black), GM (12) (red), GM (22) (green), GM (34) (blue), and GM (68) (cyan) from 0 to 10^4 Oe. GM (0), GM (12), GM (22), GM (34), and GM (68) refer to the growth media supplemented with 0 μM, 12 μM, 22 μM, 34 μM, and 68 μM Fe^{3+}, respectively.

The remanence ratios of M_r to M_s (M_r/M_s) are shown in Fig. 17c and summarized in Table 1. The theoretical M_r/M_s value for randomly oriented, non-interacting single-domain particles with uniaxial anisotropy[55] is 0.5. Mr/Ms values between 0.45 and 0.5 have been reported for other MTB strains[73]. In this study, the value of M_r/M_s was approximately 0.5 in all MS-1 cells, regardless of the initial concentration of Fe^{3+}, suggesting a random distribution of uniaxial chains composed of single-domain particles.

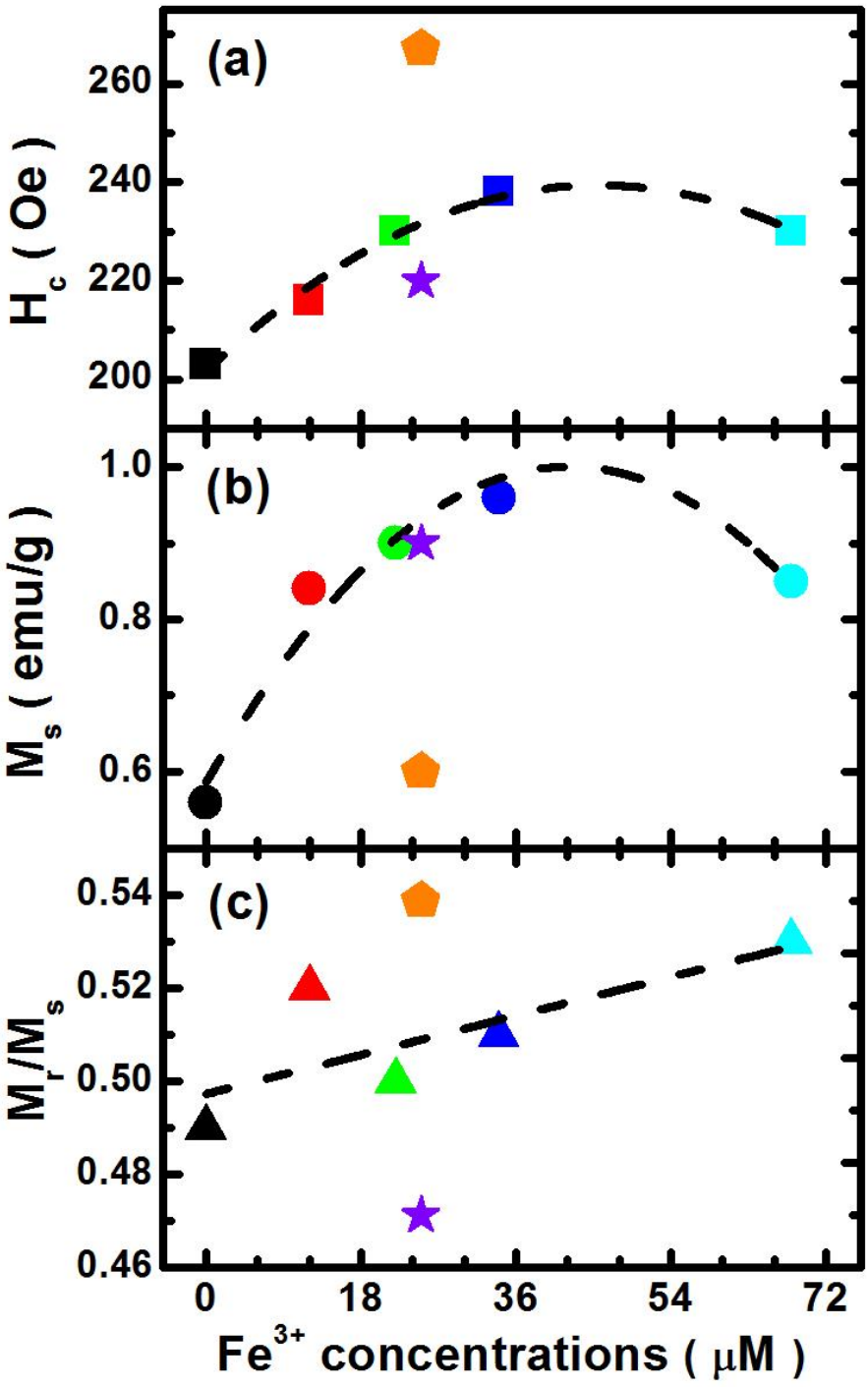

Fig. 17 Magnetic properties of *M. magnetotacticum* MS-1 cells grown at various initial concentrations of Fe^{3+}. The coercivity (H_c), the saturation magnetization (M_s), and M_r/M_s are shown in (a), (b), and (c), respectively. Previously reported data are indicated with stars[52] or pentagons[53] .

3.1.3 Temperature dependence of magnetization

The magnetization versus temperature curves for MS-1 cells, obtained in the ZFC and FC modes, are shown in Fig. 18. The FC curves of MS-1 dropped between 110 K and 80 K (Fig.18), similar to that of chemically synthesized Fe3O4 particles, which represents a transformation from cubic (above 120 K) to monoclinic (below 120 K) crystals[69]. This crystal transformation is known as the Verwey transition, and the temperature at which it occurs is known as the Verwey transition temperature (T_V). The T_V of MS-1 cells was determined based on the peak of the first-order derivative of the FC curve (inset of Fig. 18a and b). The observed minimum value of T_V was 88 K, for cells grown in GM(0), similar to that of RS-1 (T_V = 86 K)[70]. The T_V of MS-1 cells grown at other initial Fe^{3+} concentrations was approximately 95 K, similar to previously reported values (Fig. 19 and Table 10)[55]. These results suggest that the Fe_3O_4 crystals structure did not depend on the initial Fe^{3+} concentration, except in the case of GM(0).

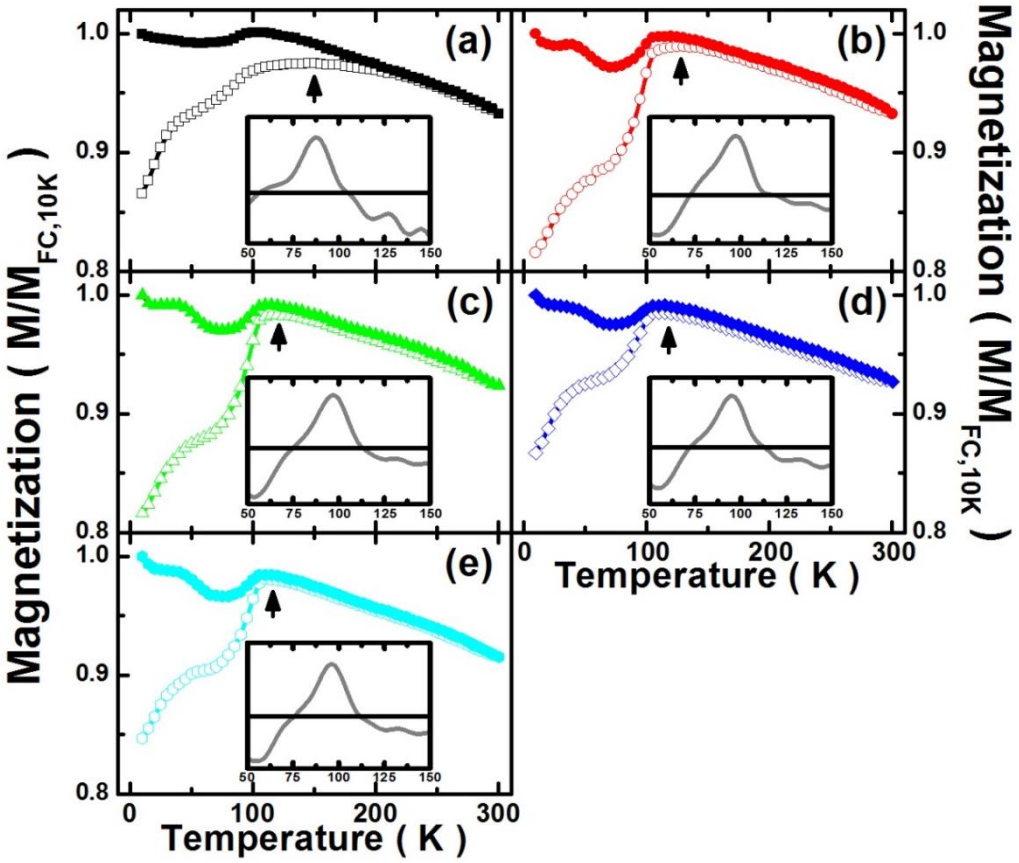

Fig. 18 Magnetization curves of ZFC (open) and FC (solid) at 1000 Oe for *M. magnetotacticum* MS-1 cells grown in GM (0) (a), GM (12) (b), GM (22) (c), GM (34) (d), and GM (68) (e). The measurements were performed at temperatures from 10 to 300 K. The Verwey transition temperature (T_V) was defined as the temperature at the peak of the first-order derivative of the FC curve (inset; gray line). The temperature at the peak of the ZFC curve was defined as the blocking temperature (T_B) (arrow). GM (0), GM (12), GM (22), GM (34), and GM (68) refer to the growth media supplemented with 0 μM, 12 μM, 22 μM, 34 μM, and 68 μM Fe^{3+}, respectively.

The ZFC curves (10-100 K) showed that magnetization of MS-1 increased as the temperature increased. Above 100 K, the magnetization tended to saturate, and then slowly declined. The temperature at the peak of the ZFC curve, indicated with an arrow in Fig. 18, corresponds to the blocking temperature, T_B, which was defined as the temperature at the transition between the blocked and the superparamagnetic states. The T_B of MS-1 cells decreased as the initial Fe^{3+} concentration increased (shown as open squares

in Fig. 19) and became constant at 34 - 68 μM. According to Prozorov *et al*.[69], when $T_V < T_B$, nanoparticles form a chain structure. The T_V value (88 - 97 K) was always smaller than the T_B value (110-150 K), suggesting that the magnetosomes of MS-1 cells grown at different initial concentrations of Fe^{3+} were arranged as chain structures in vivo.

The largest value of T_B (150 K) was observed in cells grown in GM(0). Posfái *et al*.[70] suggested that γ-Fe_2O_3 might be present in magnetite crystals produced by RS-1. If γ-Fe_2O_3 could be doped and/or coexist with magnetite in cells grown in GM(0), it would explain the large T_B values observed, because the T_B value of γ-Fe_2O_3 is nearly 200 K at 1000 Oe[90, 91]. Our results might suggest that MS-1 cells may produce γ-Fe_2O_3 as an intermediate or a byproduct in the course of magnetite formation in vivo at low concentrations of Fe^{3+} and that γ-Fe_2O_3 disappears as the Fe^{3+} concentration increases.

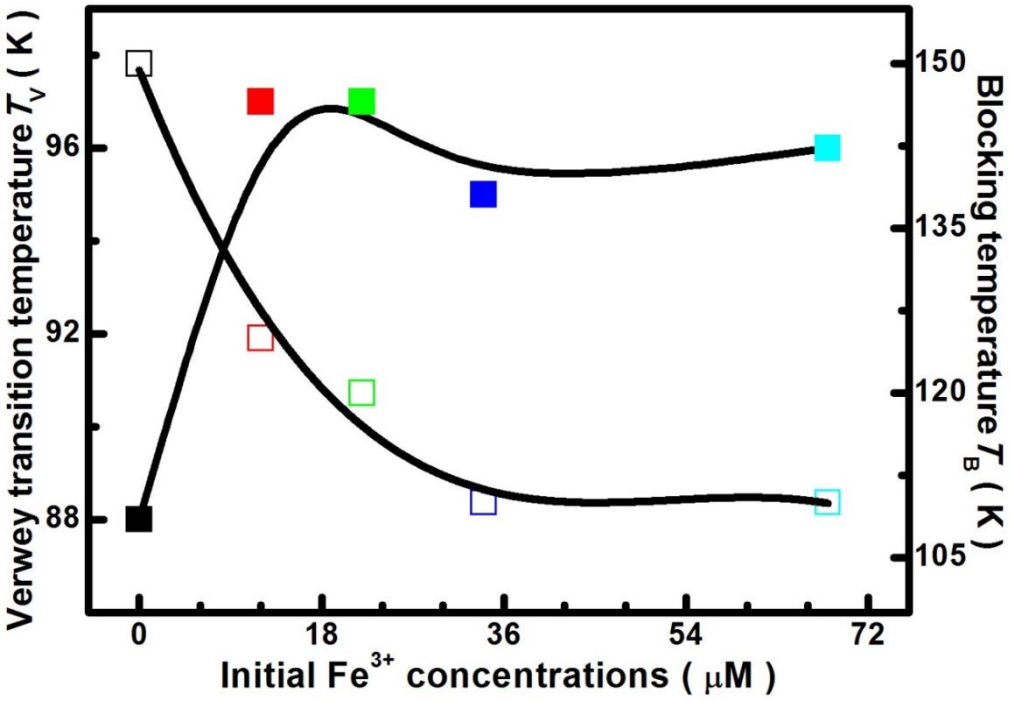

Fig. 19 The Verwey transition temperature (T_V, solid squares) and the blocking temperature (T_B, open squares) of M. magnetotacticum MS-1 cells grown at different initial concentrations of Fe^{3+}.

3.1.4 Conclusions

The yield of MS-1 cells grown at various initial concentrations of Fe^{3+} was investigated, and their magnetic properties were measured by MPMS. Although the total yield of MS-1 cells was independent of the initial Fe^{3+} concentration, the yield of magnetic cells increased as the initial Fe^{3+} concentration increased. $T_V < T_B$ in all samples, suggesting that magnetosomes were aligned in chains, regardless of the initial Fe^{3+} concentration. The maximum H_c and M_s values were observed in cells grown at 34 μM Fe^{3+}. The Verwey transition temperature of MS-1 cells grown in GM(0) differed from that of cells grown at higher initial concentrations of Fe^{3+}. A detailed study of this phenomenon might elucidate the process of magnetosome formation or transformation of iron ions in bacterial cells.

3.2 Influence of transition metal (Fe/Zn/Co) on the cells growth of *Magnetospirillum magnetotacticum* MS-1

MTB strain MS-1, AMB-1 and MSR-1 contains highly pure crystal of magnetite (Fe_3O_4) which is surrounded by 3-4 nm phospholipid bilayer in cell, which is called “magnetosome”. A diameter of magnetosome crystals are typically 35-120 nm long and morphology exposes cubo-octahedral crystal *in vivo*, which makes them single magnetic domain crystal. Therefore, applications of magnetite of MTB are limited by their own characteristics such as narrow size distribution, high purity *etc*.

Recently, the transition metals (Mn. Co, Ni, Cu, Zn *etc*.) doped into the MTB cells resulted in the magnetic properties such as H_c, T_V *etc*. are altered have been published[58, 77, 79, 80]. These altered can be broadening the application of MTB. However, they examined the magnetic properties of the

whole (or intact) cells or magnetosome levels, but the magnetite level was barely.

The details of the magnetic properties of each level with Fe, Fe/Zn or Fe/Co were described in this part. For the aims of this part, we cultured *M. magnetotacticum* MS-1 with growth medium containing Fe, Fe/Zn or Fe/Co, and the finally metal concentrations set to 34 μM. The growth status, morphology of magnetosome, magnetic properties of each level sample and analysis of metal element were presented. Details of the analytical results are described in the following sections.

3.2.1 Bacterial growth

Figure 20 shows the time course of the growth of MS-1 cells grown in the three different cultural media. The cell growth can be divided into three phases (Fig. 20a). The cells grew with a lag phase (0-60 h), an exponential phase (60-120 h) and finally reached in the stationary phase (120-168 h). The cell growth rate was not affected with Zn or Co in the culture media. Therefore, we measured the amount change of magnetic and non-magnetic cells (Fig. 20b and c). The amount of magnetic cells began to increase during an exponential phase and still increased in stationary phase, suggesting that cells uptake iron (Fig. 20b). Whether the growth rate was not different on three culture media before 120 h, the increase in the amount of magnetic cells with Zn or Co was smaller than that without them. The change in the amount of non-magnetic cells was shown in figure 20c. Figure 20d shows the ratio of the magnetic cells to the total cells. Nearly 30~40% of the total cells were magnetic. Comparing the amount of the magnetic cells (Fig. 20b and d) the amount of the magnetic cell were less in the culture with Zn or Co than that with only Fe, suggesting that Zn or Co affects the absorption process of Fe ions from the environment.

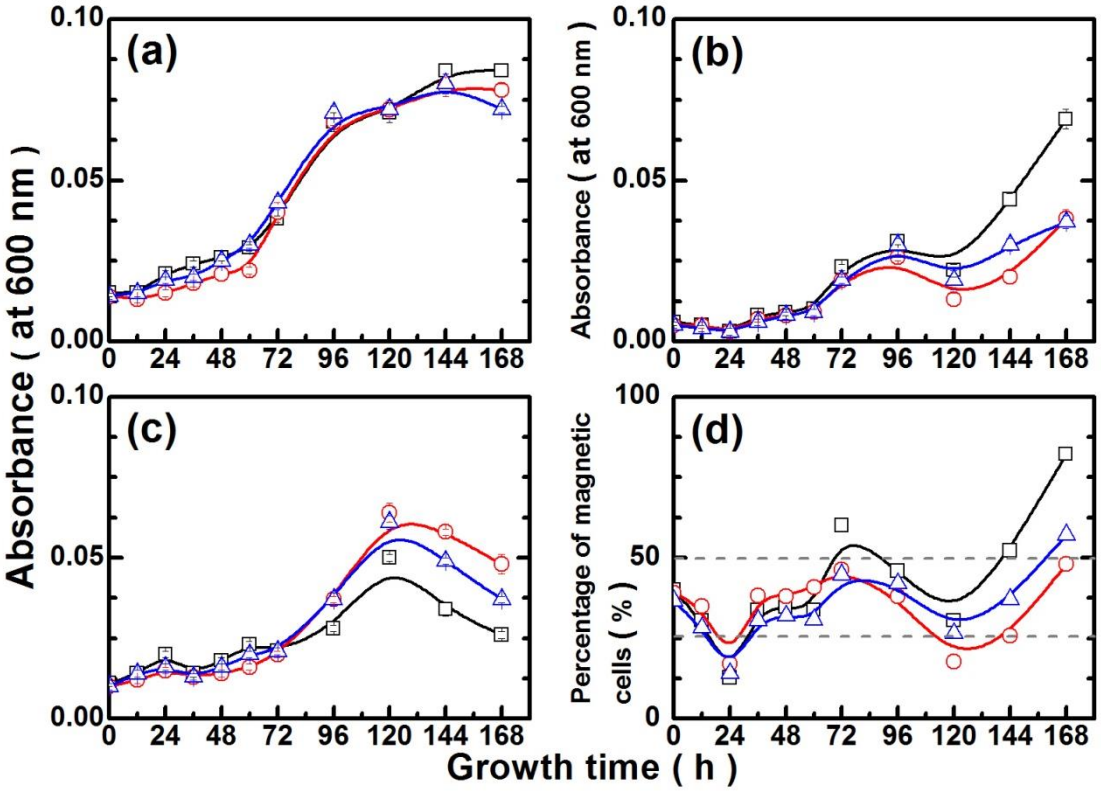

Fig. 20 The *M. magnetotacticum* MS-1 cells grown in Fe (black), Fe/Zn (red), and Fe/Co (blue) growth medium. The growth curve of total cells, and the amount of the magnetic cells and non-magnetic cells were shown in figure (a), (b) and (c), respectively. (d) The ratio of magnetic cells to total cells (weight of magnetic cells/weight of total cells × 100).

3.2.2 Magnetosome formation and grain size analysis

Magnetosomes formation of MS-1 in growth medium with Fe, Fe/Zn or Fe/Co preliminary identified by a magnet outside the screw capped bottle, and area closely the magnet appeared a black spot. The black area indicated the magnetosomes produced by MS-1 *in vivo*.

After the culture, at the stationary phase, the magnetosome in cells was observed by using TEM. The magnetosomes were completely formed and they were arranged in chain structure in growth medium with Fe, Fe/Zn or Fe/Co (Fig. 21). The grain size and shape factor of magnetosome is showed in

Fig. 22. Distribution of grain size of the Fe was 40-65 nm, yet this value range is changed in growth medium by doping with Zn (30-70 nm) or Co (30-50 nm), suggesting that Zn or Co element effect on the magnetosome formation. The average grain size of magnetosomes of MS-1 grown in Fe, Fe/Zn and Fe/Co culture was 55 nm, 48 nm and 42 nm, respectively. These results consistent with a common size of magnetosome (35-120 nm)[78]. The grain size of the cells grown in Fe/Zn or Fe/Co growth medium became smaller than those in the Fe medium. However, grain size was become smaller and distributions were become wider when doped with Zn. The TEM data are exhibited that the grain size was significantly decreased in Zn-doped or Co-doped compared to the Fe cultures ($p < 0.001$), but reduction ratio of Co-doped was larger than that of Zn-doped (Fig. 22a). It is well know that Fe_3O_4 contains two different valence of iron (ferrous, Fe^{2+}; and ferric Fe^{3+}) which distribute two different sites (tetrahedral, A site; and octahedral, B site) in the crystal: one-third of the Fe^{3+} occupies the A site, and the B site are occupied by the two-thirds of Fe^{2+} and Fe^{3+}. The transition metal cations such as Cr^{2+}, Mn^{2+}, Co^{2+}, Ni^{2+} and Zn^{2+} is easy to substituted the Fe^{3+} and Fe^{2+} in the structure of the octahedral (B-site) of the Fe_3O_4 crystal, it can influence the properties including magnetism and grain size of the ferrites[58, 92]. Therefore, it can be explanation, the smaller ionic radius of Zn^{2+} (0.74 Å) or Co^{2+} (0.74 Å) substituted the Fe^{2+} (0.78 Å) in the B site of magnetite crystal and leaded to grain size was decreased. Our results were consistent with the previous that the averaged crystallite size or particle size was decreased with doping Zn or Co[93-96].

The nanoparticles morphology of magnetite in the each sample was kept cubo-octahedral structure, and with the shape factor (k) was approximately 1 (n = 50), and was not significant difference between Fe or Zn-doped or Co-doped cultures as shown in Fig. 22b. This result suggested the morphology was not affected on the Zn or Co doped into the magnetite *in vivo*.

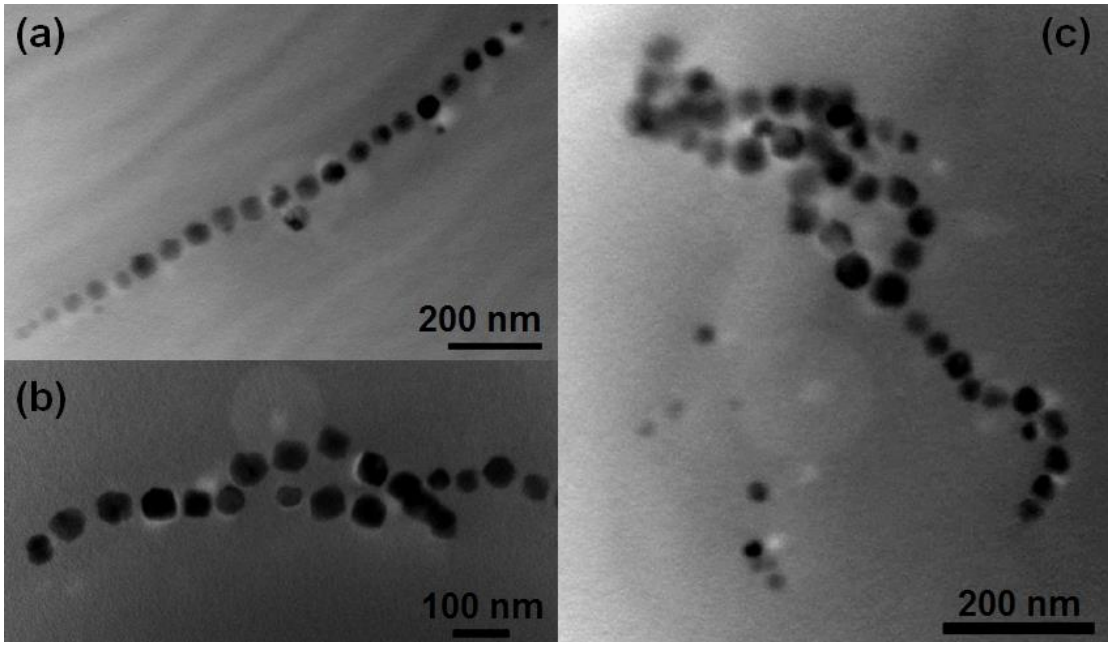

Fig. 21 Transmission electron micrograph (TEM) image of a magnetosomes chain in a cell of the *M. magnetotacticum* MS-1 cells grown in Fe (a), Fe/Zn (b), and Fe/Co (c) growth medium. The scale bars are showed inset figure. The accelerating voltage was 200 kV.

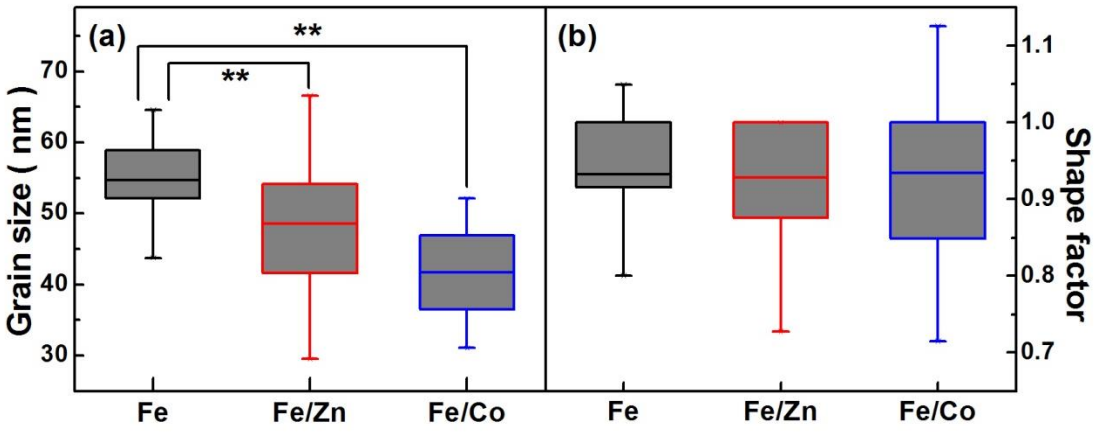

Fig. 22 Box plot is showed grain size (a) and shape factor (b) of magnetosomes of MS-1 cell grown in growth medium with Fe (black), Fe/Zn (red), and Fe/Co (blue). Grain size and shape factor of each sample was calculated as (width + length)/2 and the width to length, respectively. Statistical significance of grain size from the MS-1 cell (**, $p < 0.001$) was the comparing with grain size of Fe and Fe/Zn or Fe/Co cultures.

3.2.3 Magnetic properties analysis

Magnetic properties of intact cells (IC), magnetosomes (MG) and magnetite (MT) in MS-1 cells grew in growth medium with transition metal (Fe/Zn/Co) as showed in the following subsections.

3.2.3.1 Intact cell, magnetosome and magnetite with Fe

The hysteresis loops of IC, MG and MT in growth medium with only Fe were represented in Fig. 23a and the parameters of magnetic properties were summarized in Table 11. The magnetization of each sample was normalized with their dry weight. The saturation hysteresis loops showed, the value of M_s was significantly different with each sample (Fig. 23a and Table 11). The M_s value of IC and MG was 1.4 and 19.2 emu/g, respectively. The M_s value of MS-1 cells grown at 25 μM Fe^{3+} was reported to be 0.9 emu/g in IC or 13 emu/g in MG[52]. Our results are larger than the previous study[52]. It might be explained by different Fe^{3+} concentration in the growth medium. The M_s value of MT was larger than approximately 3 times of the MG, 59.9 emu/g. M_s value of MT reported here is consistent with that in artificially synthesized Fe_3O_4 (M_s = 65.4 emu/g when crystal size is 55 nm)[89]. The magnetosome chain in the cell reveals single magnetic domain[97]. Therefore, the freedom magnetic moment was decreased in the IC level. Conversely, the freedom magnetic moment was increased in the MG level, and magnetic moment was fully freedom in the MT level. This caused by the different M_s value in the different level.

The hysteresis loops of each sample were enlarged and showed in Fig. 23b-d. The hysteresis loops of IC, MG and MT were closed at approximately 600, 400 and 300 Oe, respectively. The ratio of M_r/M_s in IC was 0.52, suggesting a random distribution of uniaxial chains composed of single magnetic domain particles. However, M_r/M_s value of MG and MT was lower

than 0.3. The uniaxial chain may be disrupted in MG and MT level and lead to the low M_r/M_s. M_r/M_s values of whole cells between 0.43 and 0.53 have been reported for the MS-1 cells[52, 53, 55, 72]. The M_r/M_s value of IC in our study is consistent with a previous study.

The H_c value of IC was larger than that of MG and MT, and value of them was 275.5, 69.2 and 24.0 Oe, respectively. H_c value of IC and MG was larger than that of the previous study[52, 53, 58, 77]. However, the H_c of MT was virtually not reported. H_c value depends on magnetic particle characteristics such as grain size, crystal defects, and/or magnetic interactions *in vivo* [65, 87]. Because of the different forms (IC, MG and MT) of the same sample was measured, so the effected of grain size, crystal defects *etc*. was limited. The different H_c value of IC, MG and MT might cause by the magnetic interactions that were including intrachain, interchain and intercell interactions. The magnetization of IC to zero, the magnetic force (*i.e.*: applied field) was required to overcome the above three interactions. This lead to the H_c value of IC was largest. For the MG, the magnetic force is required to overcome the intrachain and interchain interactions. Hence, H_c value of MG was lower than that of IC. The reason of the smallest H_c value of MT, the magnetic force is required to overcome only interparticle interaction. The relationship of M_r/M_s and H_r/H_c is showed in Fig. 24. The IC, MG and MT samples distributed within the SD, PSD and MD+SPM region, respectively. This result can provide evidence for explanation before.

Table 11 Parameters of magnetic properties of intact cells (IC), magnetosome (MG) and magnetite (MT) with Fe

Level	M_S (emu/g)	M_r/M_s	H_c (Oe)	H_r/H_c	T_V (K)	T_B (K)
IC	1.4	0.52	275.5	1.2	95	105
MG	19.2	0.24	69.2	3.1	96	110
MT	59.9	0.10	24.0	6.9	91	105

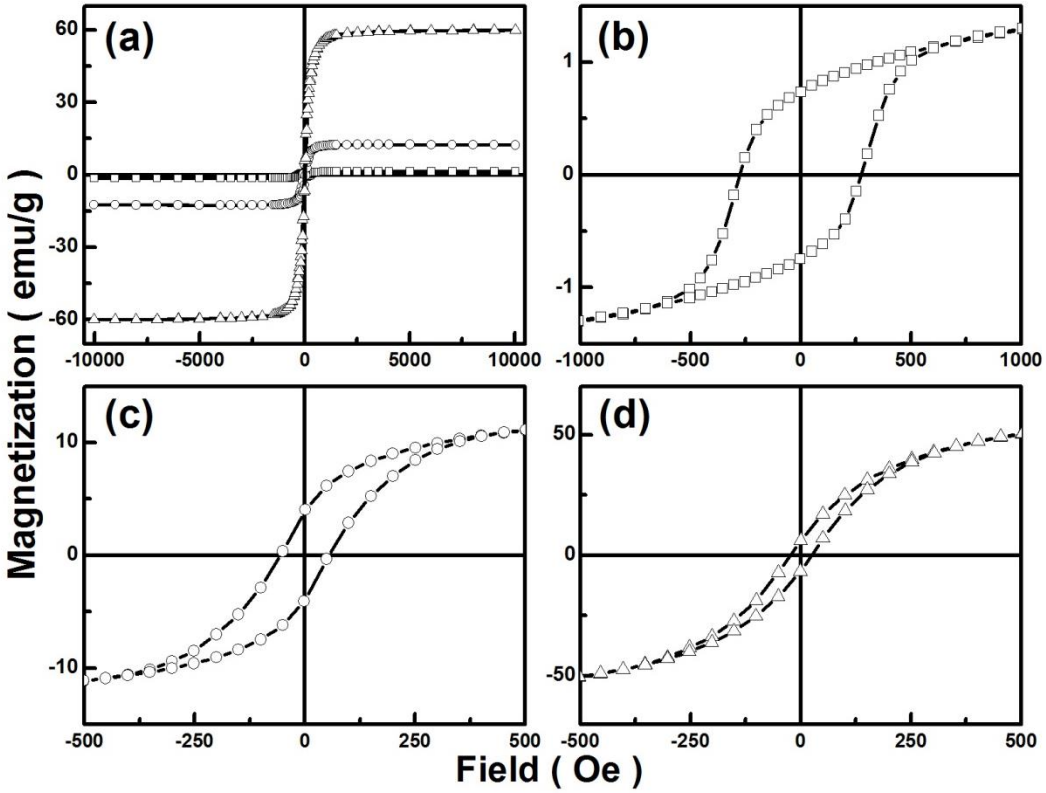

Fig. 23 Hysteresis loops of *M. magnetotacticum* MS-1 cells grown in Fe growth medium was measured at 300 K (a). The range of applied field was between -10^4 and 10^4 Oe. The hysteresis loops of intact cell (b, square), magnetosome (c, circle) and magnetite (d, triangle) were enlarged.

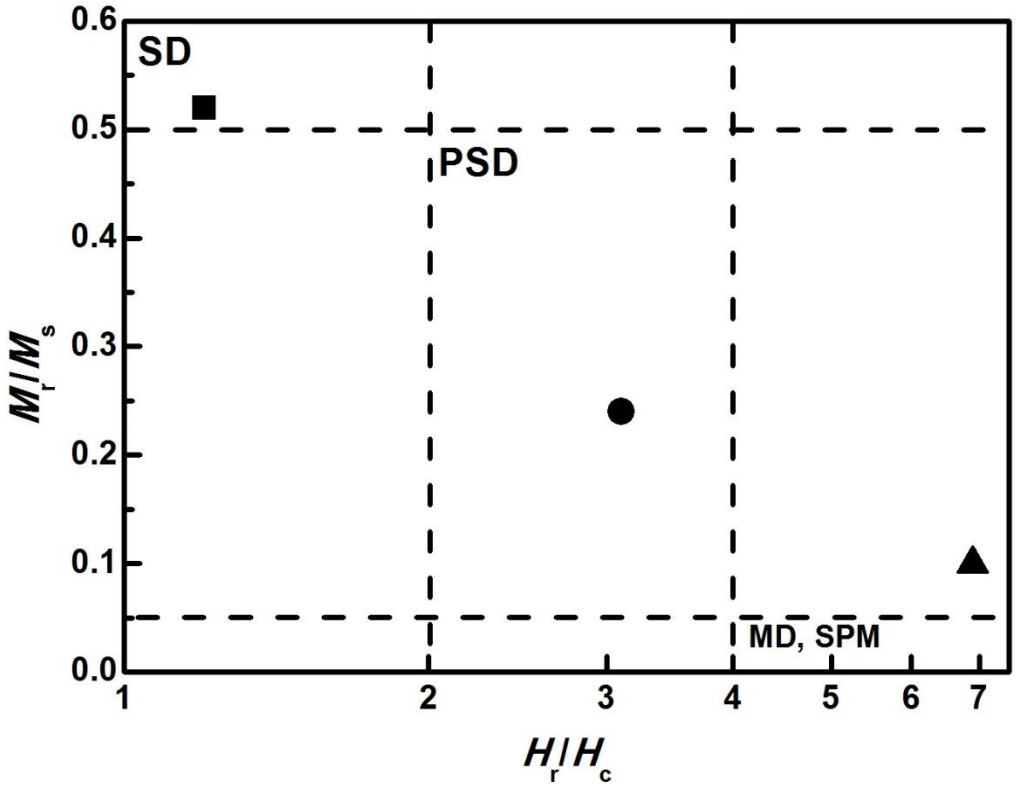

Fig. 24 Day plot of the relationship of the hysteresis loop parameters. The intact cell (IC, square), magnetosome (MG, circle) and magnetite (MT, triangle) showed in figure. Domain state regions represent typical parameter range for single domain (SD), pseudo-single domain (PSD), multi-domain (MD), and superparamagnetic (SPM) behavior.

The ZFC (open) and FC (solid) curves for IC (square), MG (circle) and MT (triangle) of MS-1 cells grown in growth medium with only Fe are presented in Fig. 25a. The figure shows, FC and ZFC curves of IC, MG and MT were appeared a peak at approximately 100 K, and below this, ZFC and FC curves were separated. This phenomenon follows from large magnetic irreversibility below the transition due to larger magnetocrystalline anisotropy. However, the variation tendency of MT was different with others below 100 K. Prozorov *et al*.[69] reported the Verwey transition in several strain MTB and agarose magnetite. Curve changes of agarose magnetite were slower than that of MTB. They found it due to the magnetocrystalline anisotropy. According to this, we can explanation, the magnetosome chain has large magnetocrystalline anisotropy than an individual one, it due to the different change between IC or

MG and MT. The T_V of IC (solid square), MG (solid circle) and MT (open triangle) was determined based on the peak of the first-order derivative of the FC curve and showed in Fig. 25b (peak enlarged inset). The value of T_V of each sample was not significantly different, 91-95 K. Our result is consistent with the previous study[55, 58]. The temperature at the peak of the ZFC curve, indicated T_B and showed in Fig. 25c (the peak of ZFC enlarged inset). The ZFC of IC (open square) and MG (open circle) showed a sharp change, but MT (solid triangle) was slower than the others. The difference between IC or MG and MT was due to the magnetocrystalline anisotropy. The value of T_B showed slightly higher than that of T_V, it ranged from 105 to 110 K. The magnetization dependence of temperature results suggested that magnetosome form a chain structure, however, this confirmation method may net appropriate for the MT sample.

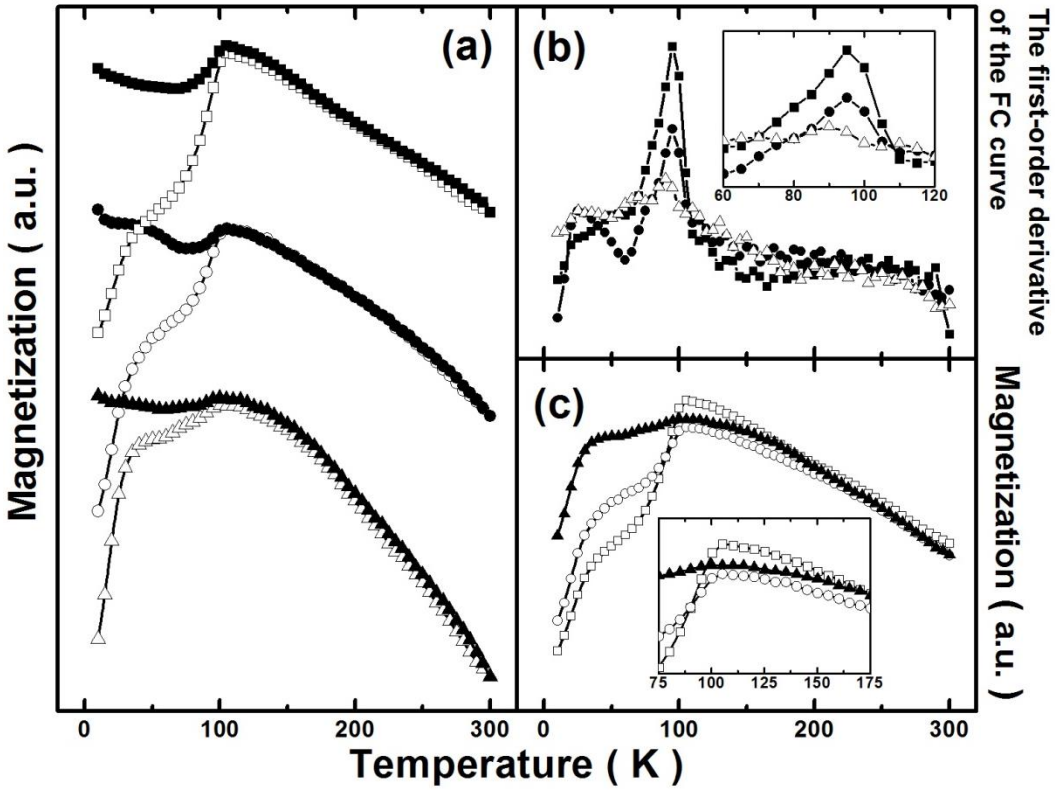

Fig. 25 Magnetization curves of ZFC (open) and FC (solid) at 1000 Oe for *M. magnetotacticum* MS-1 cells grown in Fe growth medium is showed in Fig. a. (b) The Verwey transition temperature (T_V) is defined as the temperature at

the peak of the first-order derivative of the FC curve: intact cell (IC; solid square), magnetosome (MG; solid circle) or magnetite (MT; open triangle), and the peaks are enlarged from 60 K to 120 K (inset). (c) The temperature at the peak of the ZFC curve is defined as the blocking temperature (T_B): IC (open square), MG (open circle) or MT (solid triangle), and inset figures are enlarged the ZFC peak (range: 75-175 K). The measurements were performed at temperatures from 10 to 300 K.

3.2.3.2 Intact cell, magnetosome and magnetite doping with Zn

The hysteresis loops of IC, MG and MT in growth medium doping with Zn are represented in Fig. 26a. The magnetization of each sample was normalized with their dry weight. The hysteresis loops saturated at low field (< 2000 Oe) and the value of M_S was significantly different with each sample (Fig. 26a and Table 12). The value of M_S of IC, MG and MT was 1.0, 8.6 and 31.7 emu/g, respectively. The value of M_S in our result was larger than the value that of the previous studies[77]. The difference of M_S value in these three samples is caused by the different number of magnetic moment as above explanation (section 3.2.3.1). The M_S value of each sample of MS-1 cells grown in growth medium doping with Zn was almost smaller than that of Fe growth medium. The M_S value difference between Zn and Fe: the M_S value was decreased 29%, 55% and 47% with IC, MG and MT samples, respectively. The chemical composition of the materials, crystal defects and crystal orientation decided on the M_S value. The decrease M_S value can explain the different concentration of Zn element doped into the IC, MG or MT samples. This result suggested, a lot of Zn element consisted of MG and MT level *in vivo*. The result of MG is consistent with previous studied[96, 98].

Coercivity (H_C) of IC, MG and MT are showed in Fig. 26b-d. H_C value decreased with cells separation of IC, MG and MT. H_C value of IC and MG was not significantly different with that of only Fe culture. But, H_C value of MT was

larger than that of Fe culture, 44.5 Oe. It might be explain, the Zn element doped into the crystal in the MT level, and the Zn ions existed in the IC and MG level. The different H_c value of IC, MG and MT might cause by the magnetic interactions as Section 3.2.3.1 explanation. The remanence ratios of M_r to M_s (M_r /M_s) versus ratios of H_r to H_c (H_r/H_c) plot are showed in Fig. 27 and data are summarized in Table 12. The ratio of M_r/M_s in IC was 0.51, which was same as the Fe culture, suggesting that a random distribution of uniaxial chains composed of single magnetic domain particles. However, M_r/M_s value of MG and MT was lower than 0.3, which is consistent with only Fe culture. The IC, MG and MT samples distributed within the SD, PSD and MD+SPM region, respectively. The results were similar to the only Fe culture, which suggested the Zn element significantly affected on the magnetic properties of M_s.

Table 12 Parameters of magnetic properties of intact cells (IC), magnetosome (MG) and magnetite (MT) with Zn-doped

Level	M_s (emu/g)	M_r/M_s	H_c (Oe)	H_r/H_c	T_V (K)	T_B (K)
IC	1.0	0.51	277.7	1.2	95	148
MG	8.6	0.26	65.5	3.1	96	160
MT	31.7	0.14	44.5	4.4	95	102

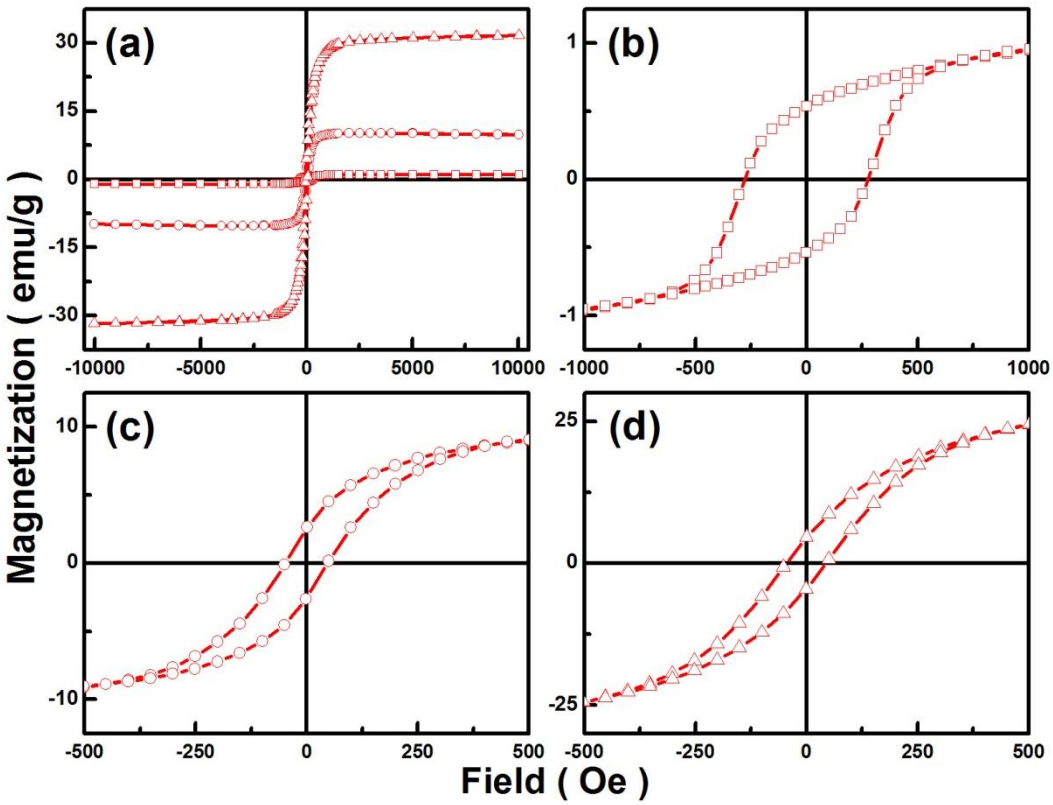

Fig. 26 Hysteresis loops of *M. magnetotacticum* MS-1 cells grown in Zn-doped growth medium was measured at 300 K (a). The range of applied field was between -10^4 and 10^4 Oe. The enlarged hysteresis loops of intact cell (IC; square), magnetosome (MG; circle) and magnetite (MT; triangle) are showed in Fig. b-d.

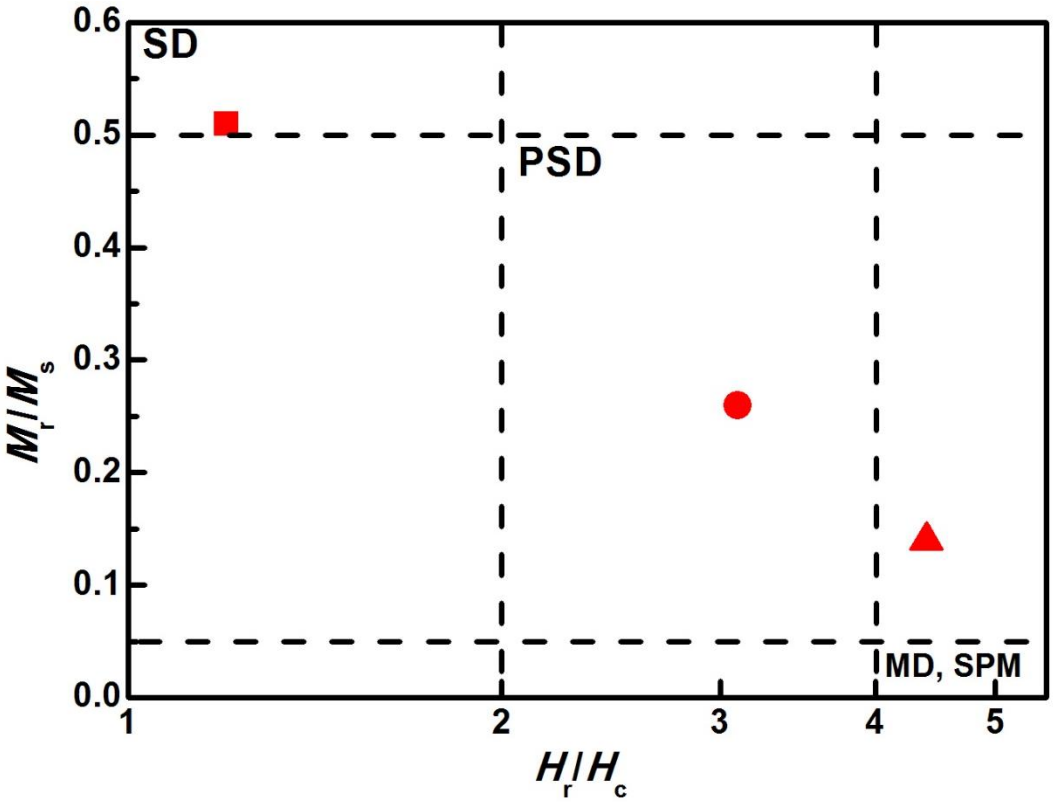

Fig. 27 Day plot of the relationship of the hysteresis loop parameters. The intact cell (IC, square), magnetosome (MG, circle) and magnetite (MT, triangle) showed in figure. Domain state regions represent typical parameter range for single domain (SD), pseudo-single domain (PSD), multi-domain (MD), and superparamagnetic (SPM) behavior.

The ZFC (open) and FC (solid) curves for IC (square), MG (circle) and MT (triangle) of MS-1 cells grown in growth medium doping with Zn are presented in Fig. 28a. The figure shows, FC curves of IC, MG and MT are appeared a peak at approximately 100 K, but the peak of ZFC curves was higher than the FC curves. The first-order derivative of the FC curves of IC (solid square), MG (solid circle) and MT (open triangle) are showed in Fig. 25b (the peak enlarged inset). The value of T_V of each sample was not significantly different, approximately 95 K (Fig. 25b and Table 12). The T_V value of IC, MG and MT of MS-1 cells grown in growth medium with doping Zn was consistent with that of the only Fe culture. The temperature at the peak of the ZFC curve, indicated T_B and showed in Fig. 25c (the peak of ZFC enlarged inset). The peak of ZFC

of IC (square) and MG (circle) was 148 and 160 K, respectively, but MT was lower than both, 102 K. The difference between IC or MG and MT was due to the magnetocrystalline anisotropy. The ZFC of MT appeared the two peaks; the low temperature peaks have no reasonable explanation. It might be the size of the magnetite caused uneven. The IC and MG, T_B almost larger than the T_V, suggesting the magnetosome magnetite arranged chain structure. Nonetheless, it was unclear for the MT level. The results suggested the diamagnetic Zn element not affected the crystal structure transition.

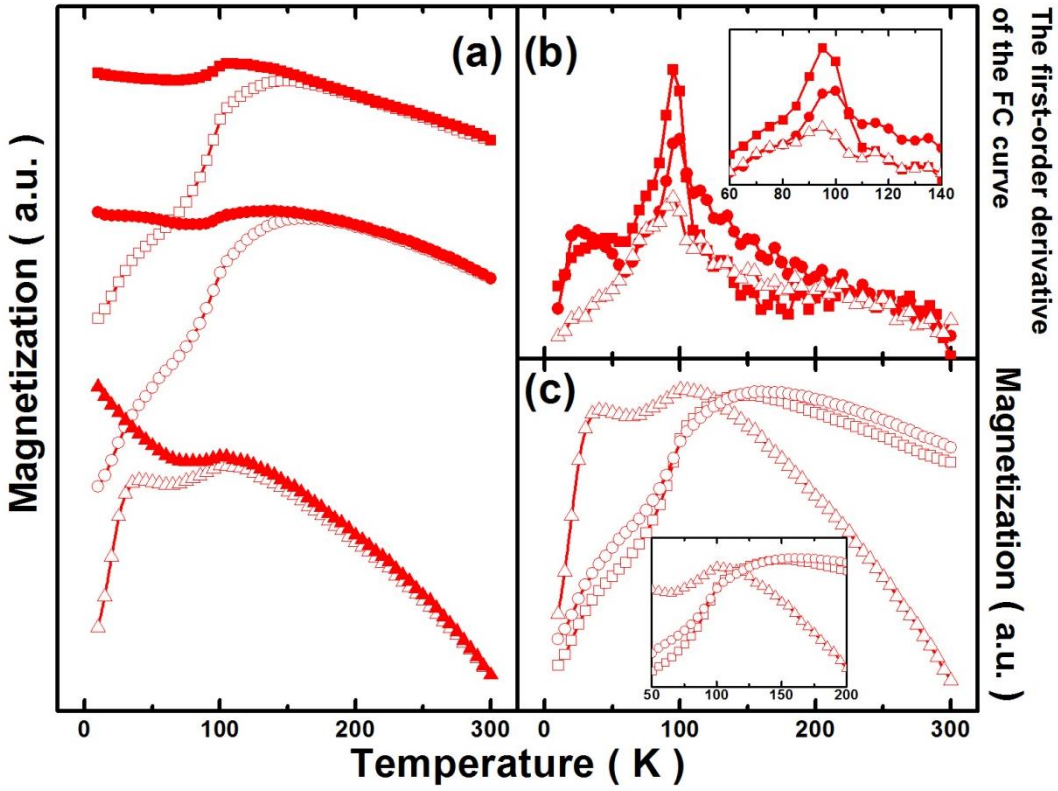

Fig. 28 (a) The ZFC (open) and FC (solid) of *M. magnetotacticum* MS-1 cells grown in Zn growth medium measured at 1000 Oe. (b) The peak of the first-order derivative of the FC curve is deemed to Verwey transition temperature (T_V): intact cell (solid square), magnetosome (solid circle) and magnetite (open triangle), and the peaks are enlarged from 60 K to 140 K (inset). (c) The temperature at the peak of the ZFC curve was defined as the blocking temperature (T_B): intact cell (open square), magnetosome (open circle) and magnetite (open triangle), and inset figure enlarged the ZFC peak (range: 50-200 K). The measurements were performed at temperatures from

10 to 300 K.

3.2.3.3 Intact cell, magnetosome and magnetite doping with Co

The change in the applied magnetic field of magnetization was showed in Figure 29. The completely hysteresis loops of IC, MG and MT in growth medium with Co were represented shows Fig. 29a. The magnetization of each sample was normalized with their dry weight. The hysteresis loops saturated at low field (< 2000 Oe). M_s value of MT was larger than that of IC (~95 times) and MG (10 times), that was 56.8 emu/g (Table 13). The difference of M_s value in these three samples is caused by the different number of magnetic moment as above explanation (section 3.2.3.1). The M_s value of IC and MG of MS-1 cells grown in growth medium with Co was smaller than that of Fe culture. The M_s value of IC and MG decreased 57% and 70%, respectively. However, M_s value of MT was not significantly different. The chemical composition of the materials, crystal defects and crystal orientation decided on the M_s value. Therefore, a lot of Co ions existed in IC and MG level *in vivo*, and a few amount Co might be doped into the crystal in MT level. It will demonstrate after section (3.2.4).

Enlarged hysteresis loops of IC, MG and MT were represented in Fig. 29b-d. The hysteresis loops closed at low field (< 1500 Oe) and displayed large H_c. That was decreased with cells separation of IC, MG and MT. H_c value of IC was achieved 357.5 Oe, and that of decreased to 240.9 and 189.2 Oe with MG and MT, respectively. The value of H_c of IC, MG and MT was all larger than that of only Fe culture. In other words, doping Co, the H_c value of IC, MG and MT was increased 30%, ~250% and ~690%, respectively. The increasing value of H_c in IC level was lower than the previous study (increased 52%)[58]. According to the M_s and H_c result, a few amount of Co element doped into the crystal in MT level resulted in slightly changing M_s and large increasing H_c. The

different H_c value of IC, MG and MT might cause by the magnetic interactions as Section 3.2.3.1 explanation. The M_r/M_s value of IC, MG and IT was reduced from 0.54 to 0.40, and the value of H_r/H_c was increased. The relation between M_r/M_s and H_r/H_c was showed in Fig. 30. The IC and MG or MT samples distributed within the SD and PSD region, respectively. The results were different to the only Fe culture, which suggested the Co element significantly affected on the magnetic properties.

Table 13 Summarized of hysteresis loops of intact cells (IC), magnetosome (MG) and magnetite (MT) with Co

Level	M_s (emu/g)	M_r/M_s	H_c (Oe)	H_r/H_c
IC	0.6	0.54	357.5	1.1
MG	5.8	0.45	240.9	2.6
MT	56.8	0.40	189.2	2.4

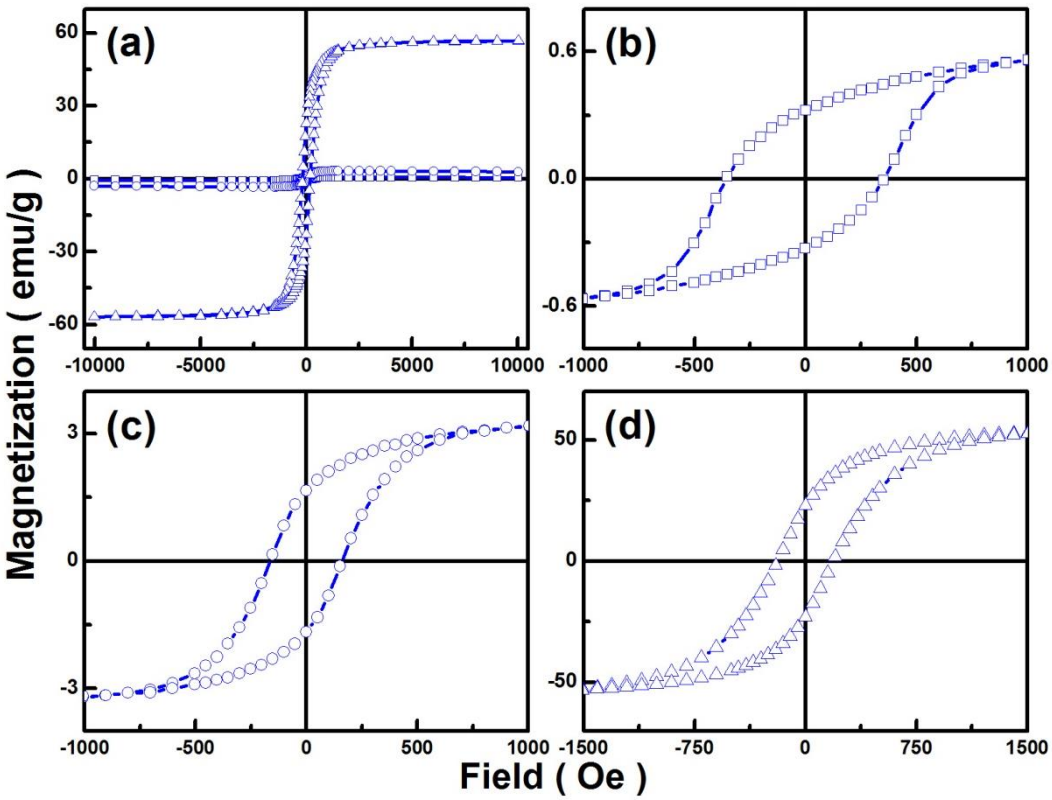

Fig. 29 Hysteresis loops of *M. magnetotacticum* MS-1 cells grown in Co growth medium was measured at 300 K (a). The range of applied field was between -10^4 and 10^4 Oe. The hysteresis loops of intact cell (b, square), magnetosome (c, circle) and magnetite (d, triangle) were enlarged.

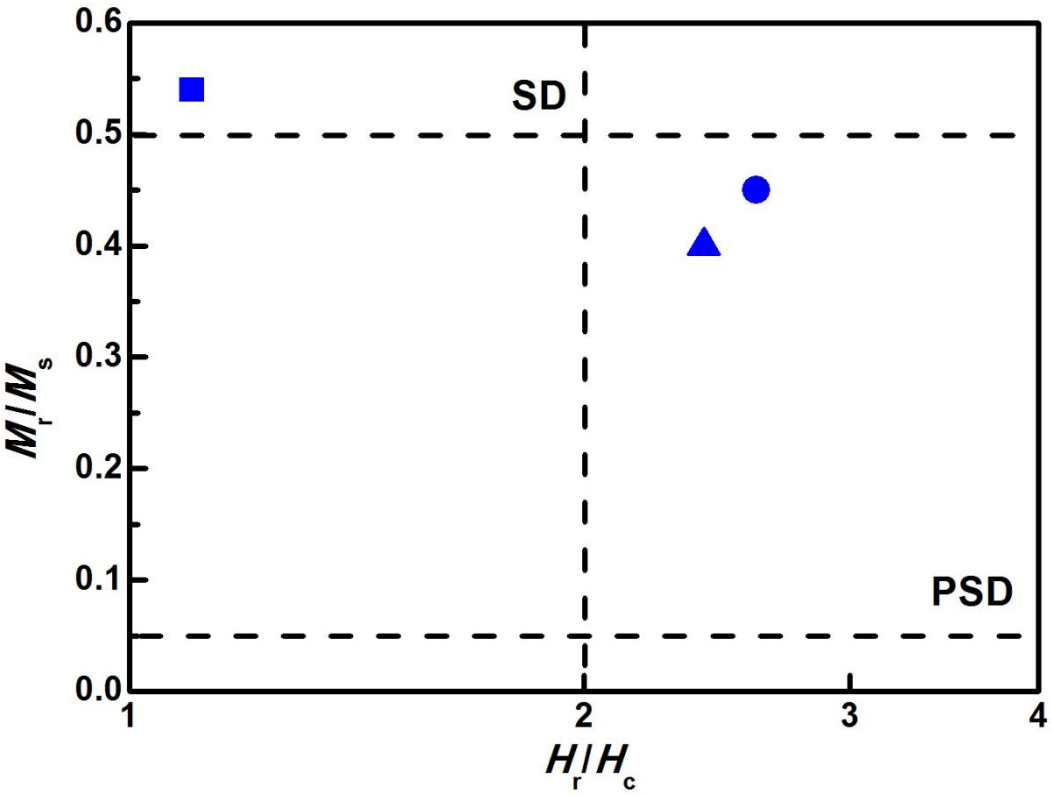

Fig. 30 Day plot of the relationship of the hysteresis loop parameters. The intact cell (IC, square), magnetosome (MG, circle) and magnetite (MT, triangle) showed in figure. Domain state regions represent typical parameter range for single domain (SD) and pseudo-single domain (PSD) behavior.

The ZFC-FC curves of IC, MG and MT of MS-1 cells grown in growth medium with doping Co were entirely different with only Fe culture (Fig. 31a). ZFC and FC curves combined at high temperature (> 250 K), and not a significant change in FC curves or almost unsaturated of ZFC curves. The first-order derivative of the FC curves did not appear the peak (Fig. 31b), which lost the Verwey transition by doping Co. It might be the ferromagnetism Co element substituted the Fe element in magnetite, which resulted in increasing

Co-Fe interaction. In the strong interaction, the crystal phase transition does not occur. Figure 31c showed the ZFC curves of IC, MG and MT. The T_B maybe appears higher temperature (> 250 K). This is consistent with the previous study[94]. The sluggish change of ZFC curves might be accounted for the above reason.

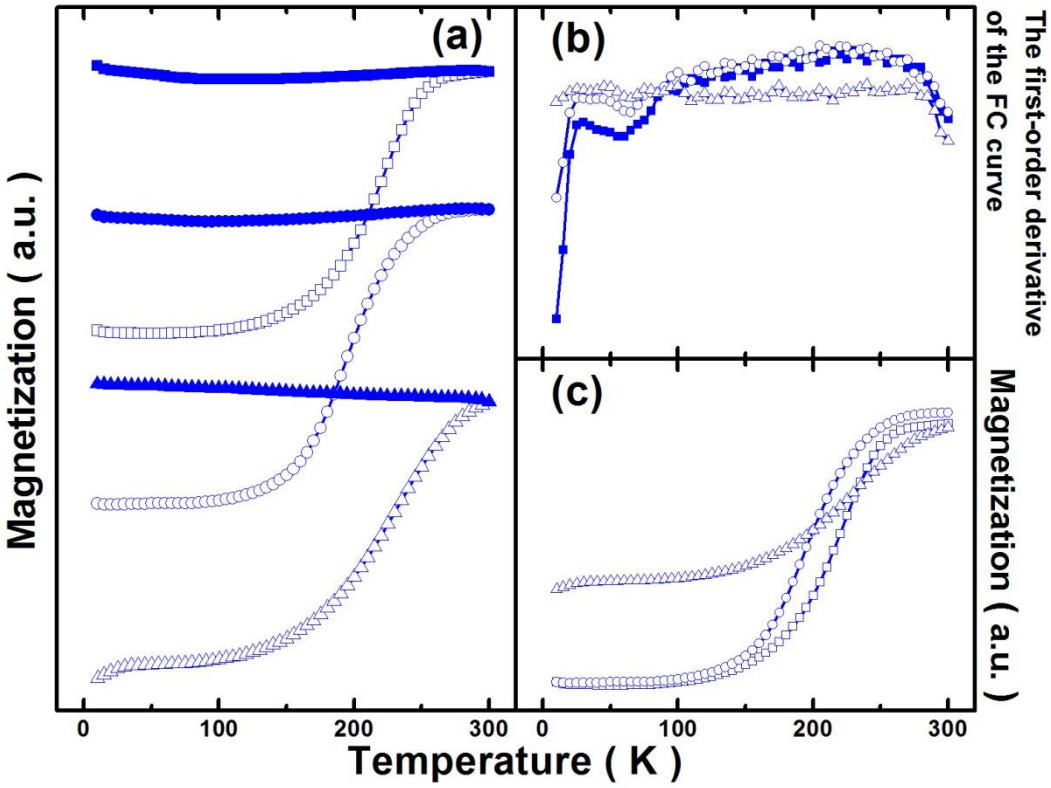

Fig. 31 Magnetization curves of ZFC (open) and FC (solid) at 1000 Oe for *M. magnetotacticum* MS-1 cells grown in Co growth medium is showed in Fig. a. (b) The peak disappeared at the first-order derivative of the FC curves: intact cell (solid square), magnetosome (solid circle) and magnetite (open triangle). (c) The ZFC curve showed the magnetization saturated at high temperature: intact cell (square), magnetosome (circle) and magnetite (triangle). The measurements were performed at temperatures from 10 to 300 K.

3.2.4 Element analysis with EPMA

The magnetic properties were significantly changed by doping Zn or Co. The

Zn or Co element in magnetosome and magnetite measured by EPMA and the results summarized in table 14. Because of the intact cells containing amount of organic compounds, so EPMA analysis is difficult.

A few amount of Zn or Co element detected in the magnetosomes magnetite. However, the concentrations of Zn or Co in the magnetosome surface were higher twice than that of magnetite (or core). This is a very good evidence to illustrate the difference of M_s in magnetosome and magnetite with doping Zn or Co. Staniland *et al*.[58] reported the Co near the surface of the magnetosome crystal than in the core. Our results are consistent with Staniland reported. The results suggesting the magnetosome membrane (or vesicle) for metal ions other than iron absorption is very demanding.

Table 14 Summarized of Zn or Co concentration in magnetosome (MG) and magnetite (MT) (at.%: atomic percentage; ×: not reported)

	Zn	Co	Co[58]	Co[58]
Transition metal in medium (μM)	12	12	10	20
MG (at.%)	0.9±0.1	1.4±0.5	0.2±0.05	1.4±0.4
MT (at.%)	0.4±0.2	0.7±0.2	×	×

3.2.5 Conclusions

Enhance the magnetic properties of magnetite synthesized by the MTB via controlling the concentrations of transition metal in the growth medium. The magnetic properties of intact cell, magnetosome and magnetite were significantly different. In my work, the first detailed description of magnetic properties of magnetite with or without doping transition metal. Magnetic behavior of magnetite synthesized by MTB is unclear. Understand this phenomenon; it is possible to further interpretation of the mechanism of

magnetosome formation.

Chapter 4 Summary

I studied the magnetic properties of magnetite synthesized by MTB strain MS-1 grown under different metal conditions. First part is about the magnetic properties of MS-1 cells grown with different concentrations of ferric (Fe^{3+}) iron and the second parts is about the magnetic properties of the intact cell, magnetosome and magnetite with doping Zn or Co.

The results of first part

1. The total yield of MS-1 cells was independent of the different initial Fe^{3+} concentrations, but the yield of magnetic cells increased with increasing initial Fe^{3+} concentrations.
2. The maximum H_c and M_s values were observed at Fe^{3+} concentration of 34 μM. The relationship between T_V and T_B ($T_V < T_B$) suggested that the magnetosomes were arranged in chain when MS-1 cells grew regardless of the initial Fe^{3+} concentration.
3. The magnetic properties of cells grown in the growth medium without addition of Fe^{3+} differed from that of cells grown at other initial concentrations of Fe^{3+}.

The above results illustrated that the Fe^{3+} concentration had marginal effect on the magnetic properties of MTB strain MS-1, except for medium without addition of Fe^{3+}. A detailed study of this phenomenon might elucidate the process of magnetosome formation or transformation of iron ions in bacterial cells.

The results of the magnetic properties of magnetite synthesized by MS-1 grown with growth medium containing Zn or Co were as follows:

1. The growth rates of the cells grown in these three media were not significantly different. The grain size of the cells grown in Fe/Zn or Fe/Co growth medium became smaller than those in the standard medium.
2. The Zn and Co affect the magnetic properties of MS-1: 2-1) The measurement of the hysteresis loops of each samples revealed that the M_S value the IC, MG and MT decreased by doping Zn, but the M_S value of magnetite was not significantly changed in MS-1 cells grown in growth medium with Co. However, Co could improve the H_C distinctly all samples; Zn did not. 2-2) By the measurement of the temperature dependence of magnetization, T_V were not significantly different in IC, MG and MT of MS-1 cells grown in the Fe and Fe/Zn growth medium. Whether T_B was larger than T_V in IC and MG of MS-1 cells grown in the Fe and Fe/Zn growth medium, suggesting that the magnetosomes were arranged in chains. But, T_B is closed to the T_V in MT at the same conditions, which suggested that the magnetosome chain is disrupted. I did not observe the T_V and T_B in all three samples of the MS-1 cells grown in the Fe/Co growth medium.
3. According to the comparison of the magnetic properties of IC and MG, the significant difference of magnetism between them would be related to the spatial arrangement of MG I the cell. For the IC, the magnetic interaction between MNPs is robust within the chain, but is weak between the chains. In the case of MG, the cell membrane disrupted and the aggregation of the chain leads to increase the magnetic interaction between the chain and

particles which in turn decreased H_c of the sample.

4. The comparison of MT and MG (or IC), the result showed the magnetic properties of MT were different to that MG (or IC) under doping Zn and Co. Under Zn conditions, the value of M_s was smaller, but H_c was larger than that under the standard conditions. Under the Co conditions, the M_s was similar and H_c was larger than the value under the standard conditions.

These results suggested that a few amount of Zn and Co was incorporated into MNPs *in vivo*.

However, magnetic behaviors of magnetite synthesized by MTB with or without doping transition metal were unclear. Moreover, magnetic properties of magnetite doping with Zn or Co appear a completely different phenomenon. This phenomenon needs to be studied in the future.

Reference

[1] Lu AH, Salabas EL, Schuth F. Magnetic nanoparticles: synthesis, protection, functionalization, and application. Angewandte Chemie International Edition English. 2007;46:1222-44.

[2] Frankel RB, Blakemore RP, Wolfe RS. Magnetite in freshwater magnetotactic bacteria. Science. 1979;203:1355-6.

[3] Heywood BR, Bazylinski DA, Garratt-Reed A, Mann S, Frankel RB. Controlled biosynthesis of greigite (Fe_3S_4) in magnetotactic bacteria. Naturwissenschaften. 1990;77:536-8.

[4] Mann S, Sparks NHC, Frankel RB, Bazylinski DA, Jannasch HW. Biomineralization of ferrimagnetic greigite (Fe_3S_4) and iron pyrite (FeS_2) in a magnetotactic bacterium. Nature. 1990;343:258-61.

[5] Farina M, Esquivel DMS, Lins de Barros HGP. Magnetic iron-sulphur crystals from a magnetotactic microorganism. Nature. 1990;343:256-8.

[6] Groby YA, Beveridge TJ, Blakemore RP. Characterization of the bacterial magnetosome membrane. Journal of Bacteriology. 1988;170:834-41.

[7] Bazylinski DA, Frankel RB. Magnetosome formation in prokaryotes. Nature Reviews Microbiology. 2004;2:217-30.

[8] Blakemore RP, Maratea D, Wolfe RS. Isolation and pure culture of a freshwater magnetic spirillum in chemically defined medium. Journal of Bacteriology. 1979;140:720-9.

[9] Bellini S. Su di un particolare comportamento di batteri dacqua dolce. 1963.

[10] Blakemore R. Magnetotactic bacteria. Science. 1975;190:377-9.

[11] Matsunaga T, Sakaguchi T, Tadakoro F. Magnetite formation by a magnetic bacterium capable of growing aerobically. Applied Microbiolog and Biotechnology. 1991;35:651-5.

[12] Schüler D, Baeuerlein E. Iron transport and magnetite crystal formation of the magnetic bacterium *Magnetospirillum gryphiswaldense*. Journal de Physique Archives. 1997;07:647-50.

[13] Sakaguchi S, Burgess JG, Matsunaga T. Magnetite formation by a sulphate-reducing bacterium. Nature. 1993;365:47-9.

[14] Moench TT. Bilophococcus magnetotacticus gen. nov. sp. nov., a motile, magnetic coccus. Antonie Van Leeuwenhoek. 1988;54:483-96.

[15] Bazylinski DA, RB; F, Jannasch HW. Anaerobic magnetite production by a marine, magnetotactic bacterium. Nature. 1988;334:518-9.

[16] Meldrum FC, Mann S, Heywood BR, Frankel RB, Bazylinski DA. Electron microscopy study of magnetosomes in two cultured vibrioid magnetotactic bacteria. Proceedings of the Royal Society of London Series B-Biological Sciences. 1993;251:237-42.

[17] Schüler D. Formation of magnetosomes in magnetotactic bacteria. Journal of Molecular Microbiology and Biotechnology. 1999;1:79-86.

[18] Calugay RJ, Okamura Y, Wahyudi AT, Takeyama H, Matsunaga T. Siderophore production of a

periplasmic transport binding protein kinase gene defective mutant of *Magnetospirillum magneticum* AMB-1. Biochemical and Biophysical Research Communications. 2004;323:852-7.

[19] Arakaki A, Nakazawa H, Nemoto M, Mori T, Matsunaga T. Formation of magnetite by bacteria and its application. Journal of The Royal Society Interface. 2008;5:977-99.

[20] Lin W, Wang Y, Li B, Pan Y. A biogeographic distribution of magnetotactic bacteria influenced by salinity. The ISME Journal. 2012;6:475-9.

[21] Yan L, Zhang S, Chen P, Liu H, Yin H, Li H. Magnetotactic bacteria, magnetosomes and their application. Microbiological Research. 2012;167:507-19.

[22] Schüler D, Frankel RB. Bacterial magnetosomes: microbiology, biomineralization and biotechnological applications. Applied Microbiolog and Biotechnology. 1999;52:464-73.

[23] Bazylinski DA, Heywood BR, Mann S, Frankel RB. Fe_30_4 and Fe_3S_4 in a bacterium. Nature. 1993;366:218.

[24] Towe KM, Moench TT. Electron-optical characterization of bacterial magnetite. Earth and Planetary Science Letters. 1981;52:213-20.

[25] Bazylinski DA, Garratt-Reed AJ, Abedi A, Frankel RB. Copper association with iron sulfide magnetosomes in a magnetotactic bacterium. Archives of Microbiology. 1993;160:35-42.

[26] Keim CN, Lins U, Farina M. Elemental analysis of uncultured magnetotactic bacteria exposed to heavy metals. Canadian Journal of Microbiology. 2001;47:1132-6.

[27] Gao J, Pan HM, Yue HD, Song T, ;, Zhao Y, Chen GJ, et al. Isolation and biological characteristics of aerobic marine magnetotactic bacterium YSC-1. Chinese Journal of Oceanology and Limnology. 2006;24:358-63.

[28] Lefevre CT, Abreu F, Lins U, Bazylinski DA. A bacterial backbone: magnetosomes in magnetotactic bacteria. Metal Nanoparticles in Microbiology: Springer; 2011. p. 75-102.

[29] Arakaki A, Webb J, Matsunaga T. A novel protein tightly bound to bacterial magnetic particles in *Magnetospirillum magneticum* strain AMB-1. Journal of Biological Chemistry. 2003;278:8745-50.

[30] Mann S, Sparks N, Blakemore R. Structure, morphology and crystal growth of anisotropic magnetite crystals in magnetotactic bacteria. Proceedings of the Royal Society of London B: Biological Sciences. 1987;231:477-87.

[31] Blakemore RP, Short KA, Bazylinski DA, Rosenblatt C, Frankel RB. Microaerobic conditions are required for magnetite formation within *Aquaspirillum magnetotacticum*. Geomicrobiology Journal. 1985;4:53-71.

[32] Schüler D, Baeuerlein E. Dynamics of iron uptake and Fe_3O_4 biomineralization during aerobic and microaerobic growth of *Magnetospirillum gryphiswaldense*. Journal of Bacteriology. 1998;180:159-62.

[33] Yang CD, Takeyama H, Tanaka T, Matsunaga T. Effects of growth medium composition, iron sources and atmospheric oxygen concentrations on production of luciferase-bacterial magnetic particle complex by a recombinant *Magnetospirillum magneticum* AMB-1. Enzyme and Microbial Technology.

2001;29:13-9.

[34] Popa R, Fang W, Nealson KH, Souza Egipsy V, Berquó TS, Banerjee SK, et al. Effect of oxidative stress on the growth of magnetic particles in *Magnetospirillum magneticum*. International microbiology. 2009;12:49-57.

[35] Heyen U, Schüler D. Growth and magnetosome formation by microaerophilic *Magnetospirillum* strains in an oxygen-controlled fermentor. Applied Microbiology and Biotechnology. 2003;61:536-44.

[36] Sun JB, Zhao F, Tang T, Jiang W, Tian JS, Li Y, et al. High-yield growth and magnetosome formation by *Magnetospirillum gryphiswaldense* MSR-1 in an oxygen-controlled fermentor supplied solely with air. Applied Microbiology and Biotechnology. 2008;79:389-97.

[37] Naresh M, Das S, Mishra P, Mittal A. The chemical formula of a magnetotactic bacterium. Biotechnology and Bioengineering. 2012;109:1205-16.

[38] Mandernack KW. Oxygen and iron isotope studies of magnetite produced by magnetotactic bacteria. Science. 1999;285:1892-6.

[39] Moench TT, Konetzka WA. A novel method for the isolation and study of a magnetotactic bacterium. Archives of Microbiology. 1978;119:203-12.

[40] Roberts AP, Florindo F, Villa G, Liao C, Jovane L, Bohaty SM, et al. Magnetotactic bacterial abundance in pelagic marine environments is limited by organic carbon flux and availability of dissolved iron. Earth and Planetary Science Letters. 2011;310:441-52.

[41] Boyd P, Ellwood M. The biogeochemical cycle of iron in the ocean. Nature Geoscience. 2010;3:675-82.

[42] Schüler D, Baeuerlein E. Iron-limited growth and kinetics of iron uptake in *Magnetospirillum gryphiswaldense*. Archives of Microbiology. 1996;166:301-7.

[43] Frankel RB, Papaefthymiou GC, Blakemore RP, W.; O. Fe_3O_4 precipitation in magnetotactic bacteria. Biochimica et Biophysica Acta. 1983;763:147-59.

[44] Leong JOHN, Neilands JB. Mechanisms of siderophore iron transport. Journal of Bacteriology. 1976;126:823-30.

[45] Paoletti LC, Blakemore. RP. Hydroxamate production by *Aquaspirillum magnetotacticum*. Journal of Bacteriology. 1986;167:73-6.

[46] Calugay RJ, Miyashita H, Okamura Y, Matsunaga T. Siderophore production by the magnetic bacterium *Magnetospirillum magneticum* AMB-1. FEMS Microbiology Letters. 2003;218:371-5.

[47] Dubbels BL, DiSpirito AA, Morton JD, Semrau JD, Neto JN, Bazylinski DA. Evidence for a copper-dependent iron transport system in the marine, magnetotactic bacterium strain MV-1. Microbiology. 2004;150:2931-45.

[48] Fukumori Y, Oyanagi H, Yoshimatsu K, Noguchi Y, Fujiwara T. Enzymatic iron oxidation and reduction in magnetite synthesizing *Magnetospirillum Magnetotacticum*. Journal de Physique Archives. 1997;07:659-62.

[49] Tamegai H, Fukumori Y. Purification, and some molecular and enzymatic features of a novel *ccb*-type cytochrome *c* oxidase from a microaerobic denitrifier, *Magnetospirillum magnetotacticum*. FEBS Letters. 1994;347:22-6.

[50] Komeili A, Li Z, Newman DK, Jensen GJ. Magnetosomes are cell membrane invaginations organized by the actin-like protein MamK. Science. 2006;311:242-5.

[51] Thomas-Keprta KL, Clemett SJ, Bazylinski DA, Kirschvink JL, McKay DS, Wentworth SJ, et al. Truncated hexa-octahedral magnetite crystals in ALH84001: presumptive biosignatures. Proceedings of the National Academy of Sciences. 2001;98:2164-9.

[52] Denham CR, Blakemore RP, Frankel RB. Bulk magnetic properties of magnetotactic bacteria. IEEE Transcations on Magnetics. 1980;16:1006-7.

[53] Moskowitz BM, Frankel RB, Flanders PJ, Blakemore RP, Schwartz BB. Magnetic properties of magnetotactic bacteria. Journal of Magnetism and Magnetic Materials. 1988;73:273-88.

[54] Moskowitz BM, Frankel RB, Bazylinski DA, Jannasch HW, Lovley DR. A comparison of magnetite particles produced anaerobically by magnetotactic. Geophysical Research Letters. 1989;16:665-8.

[55] Moskowitz BM, Frankel RB, Bazylinski DA. Rock magnetic criteria for the detection of biogenic magnetite. Earth and Planetary Science Letters. 1993;120:283-300.

[56] Weiss BP, Kim SS, Kirschvink JL, Kopp RE, Sankaran M, Kobayashi A, et al. Magnetic tests for magnetosome chains in Martian meteorite ALH84001. Proceedings of the National Academy of Sciences of the United States of America. 2004;101:8281-4.

[57] Moskowitz BM, Bazylinski DA, Egli R, Frankel RB, Edwards KJ. Magnetic properties of marine magnetotactic bacteria in a seasonally stratified coastal pond (Salt Pond, MA, USA). Geophysical Journal International. 2008;174:75-92.

[58] Staniland S, Williams W, Telling N, Van Der Laan G, Harrison A, Ward B. Controlled cobalt doping of magnetosomes *in vivo*. Nature Nanotechnology. 2008;3:158-62.

[59] Fischer H, Mastrogiacomo G, Löffler JF, Warthmann RJ, Weidler PG, Gehring AU. Ferromagnetic resonance and magnetic characteristics of intact magnetosome chains in *Magnetospirillum gryphiswaldense*. Earth and Planetary Science Letters. 2008;270:200-8.

[60] Kopp R, Weiss B, Maloof A, Vali H, Nash C, Kirschvink J. Chains, clumps, and strings: *Magnetofossil* taphonomy with ferromagnetic resonance spectroscopy. Earth and Planetary Science Letters. 2006;247:10-25.

[61] Wei J, Knittel I, Lang C, Schüler D, Hartmann U. Magnetic properties of single biogenic magnetite nanoparticles. Journal of Nanoparticle Research. 2011;13:3345-52.

[62] Simpson ET, Kasama T, Pósfai M, Buseck PR, Harrison RJ, Dunin-Borkowski RE. Magnetic induction mapping of magnetite chains in magnetotactic bacteria at room temperature and close to the Verwey transition using electron holography. Journal of Physics: Conference Series. 2005;17:108-21.

[63] Pan YX, Lin W, Tian LX, Zhu RX, Petersen N. Combined approaches for characterization of an

uncultivated *Magnetotactic coccus* from Lake Miyun near Beijing. Geomicrobiology Journal. 2009;26:313-20.

[64] Pan Y, Petersen N, Davila AF, Zhang L, Winklhofer M, Liu Q, et al. The detection of bacterial magnetite in recent sediments of Lake Chiemsee (southern Germany). Earth and Planetary Science Letters. 2005;232:109-23.

[65] Li JH, Pan YX, Chen GJ, Liu QS, Tian LX, Lin W. Magnetite magnetosome and fragmental chain formation of *Magnetospirillum magneticum* AMB-1: transmission electron microscopy and magnetic observations. Geophysical Journal International. 2009;177:33-42.

[66] Li J, Pan Y, Liu Q, Yu-Zhang K, Menguy N, Che R, et al. Biomineralization, crystallography and magnetic properties of bullet-shaped magnetite magnetosomes in giant rod magnetotactic bacteria. Earth and Planetary Science Letters. 2010;293:368-76.

[67] Pan Y, Petersen N, Winklhofer M, Davila AF, Liu Q, Frederichs T, et al. Rock magnetic properties of uncultured magnetotactic bacteria. Earth and Planetary Science Letters. 2005;237:311-25.

[68] Verwey EJW. Electronic conduction of magnetite (Fe_3O_4) and its transition point at low temperatures. Nature. 1939;144:327-8.

[69] Prozorov R, Prozorov T, Mallapragada SK, Narasimhan B, Williams TJ, Bazylinski DA. Magnetic irreversibility and the Verwey transition in nanocrystalline bacterial magnetite. Physical Review B. 2007;76.

[70] Pósfai M, Moskowitz BM, Arató B, Schüler D, Flies C, Bazylinski DA, et al. Properties of intracellular magnetite crystals produced by *Desulfovibrio magneticus* strain RS-1. Earth and Planetary Science Letters. 2006;249:444-55.

[71] Li J, Pan Y, Liu Q, Qin H, Deng C, Che R, et al. A comparative study of magnetic properties between whole cells and isolated magnetosomes of *Magnetospirillum magneticum* AMB-1. Chinese Science Bulletin. 2009;55:38-44.

[72] Yiriletu, Iwasa T. Magnetic properties of magnetite synthesized by *Magnetospirillum magnetotacticum* MS-1 cultured with different concentrations of ferric iron. Biotechnology Letters. 2015;37:2427-33.

[73] Bazylinski DA, Moskowitz BM. Microbial biomineralization of magnetic iron minerals; microbiology, magnetism and environmental significance. Reviews in Mineralogy and Geochemistry. 1997;35:181-223.

[74] Zhu K, Pan H, Li J, Yu-Zhang K, Zhang SD, Zhang WY, et al. Isolation and characterization of a marine magnetotactic spirillum axenic culture QH-2 from an intertidal zone of the China Sea. Research in Microbiology. 2010;161:276-83.

[75] Faivre D, Schüler D. Magnetotactic bacteria and magnetosomes. Chemical Reviews. 2008;108:4875-98.

[76] Alphandéry E, Ngo AT, Lefèvre C, Lisiecki I, Wu LF, Pileni MP. Difference between the magnetic properties of the magnetotactic bacteria and those of the extracted magnetosomes: Influence of the

distance between the chains of magnetosomes. The Journal of Physical Chemistry C. 2008;112:12304-9.
[77] Kundu S, Kale AA, Banpurkar AG, Kulkarni GR, Ogale SB. On the change in bacterial size and magnetosome features for *Magnetospirillum magnetotacticum* (MS-1) under high concentrations of zinc and nickel. Biomaterials. 2009;30:4211-8.
[78] Bazylinski DA. Electron microscopic studies of magnetosomes in magnetotactic bacteria. Microscopy Research and Technique. 1994;27:289-402.
[79] Tanaka M, Brown R, Hondow N, Arakaki A, Matsunaga T, Staniland S. Highest levels of Cu, Mn and Co doped into nanomagnetic magnetosomes through optimized biomineralisation. Journal of Materials Chemistry. 2012;22:11919.
[80] Prozorov T, Perez-Gonzalez T, Valverde-Tercedor C, Jimenez-Lopez C, Yebra-Rodriguez A, Körnig A, et al. Manganese incorporation into the magnetosome magnetite: magnetic signature of doping. European Journal of Mineralogy. 2014;26:457-71.
[81] Yiriletu, Watanabe S, Iwasa T. Magnetic bacteria as a tool for bioremediation of heavy metal ion. Advanced Materials Research: Trans Tech Publications; 2014. p. 589-92.
[82] Hey M. The determination of ferrous and ferric iron in rocks and minerals; and a note on sulphosalicylic acid as a reagent for Fe and Ti. Miner Magazine. 1982;46:111-8.
[83] Watanabe S, Akutagawa S, Sawada K, Iwasa T, Shimoyama Y. A ferromagnetic resonance study of iron complexes as biologically synthesized in magnetic bacteria. Materials transactions. 2009;50:2187-91.
[84] Lazić D, Škundrić B, Penavin-Škundrić J, Sladojević S, Vasiljević L, Blagojević D, et al. Stability of tris-1, 10-phenanthroline iron (II) complex in different composites. Chemical Industry and Chemical Engineering Quarterly. 2010;16:193-8.
[85] Caruntu D, Caruntu G, O'Connor CJ. Magnetic properties of variable-sized Fe_3O_4 nanoparticles synthesized from non-aqueous homogeneous solutions of polyols. Journal of Physics D: Applied Physics. 2007;40:5801.
[86] Noguchi Y, Fujiwara T, Yoshimatsu K, Fukumori Y. Iron reductase for magnetite synthesis in the magnetotactic bacterium *Magnetospirillum magnetotacticum*. Journal of Bacteriology. 1999;181:2142-7.
[87] Katzmann E, Eibauer M, Lin W, Pan Y, Plitzko JM, Schuler D. Analysis of magnetosome chains in magnetotactic bacteria by magnetic measurements and automated image analysis of electron micrographs. Applied and Environmental Microbiology. 2013;79:7755-62.
[88] Özdemir Ö, Dunlop DJ, Moskowitz BM. Changes in remanence, coercivity and domain state at low temperature in magnetite. Earth and Planetary Science Letters. 2002;194:343-58.
[89] Goya G, Berquo T, Fonseca F, Morales M. Static and dynamic magnetic properties of spherical magnetite nanoparticles. Journal of Applied Physics. 2003;94:3520-8.
[90] Wu W, Xiao X, Zhang S, Peng T, Zhou J, Ren F, et al. Synthesis and magnetic properties of maghemite (γ-Fe_2O_3) short-nanotubes. Nanoscale Research Letters. 2010;5:1474-9.

[91] Özdemir Ö, Dunlop DJ. Hallmarks of maghemitization in low-temperature remanence cycling of partially oxidized magnetite nanoparticles. Journal of Geophysical Research: Solid Earth (1978-2012). 2010;115.

[92] Byrne JM. Biogenic magnetite nanoparticles: development and optimization for potential applications. 2012;PhD thesis, University of Manchester.

[93] Shannon RD. Revised effective ionic radii and systematic studies of interatomic distances in halides and chalcogenides. Acta Crystallographica Section A: Crystal Physics, Diffraction, Theoretical and General Crystallography. 1976;32:751-67.

[94] Galloway JM, Arakaki A, Masuda F, Tanaka T, Matsunaga T, Staniland SS. Magnetic bacterial protein Mms6 controls morphology, crystallinity and magnetism of cobalt-doped magnetite nanoparticles in vitro. Journal of Materials Chemistry. 2011;21:15244.

[95] Byrne JM, Coker VS, Moise S, Wincott PL, Vaughan DJ, Tuna F, et al. Controlled cobalt doping in biogenic magnetite nanoparticles. Journal of The Royal Society Interface. 2013;10:20130134.

[96] Byrne JM, Coker VS, Cespedes E, Wincott PL, Vaughan DJ, Pattrick RAD, et al. Biosynthesis of zinc substituted magnetite nanoparticles with enhanced magnetic properties. Advanced Functional Materials. 2014;24:2518-29.

[97] Dunin-Borkowski RE. Magnetic Microstructure of Magnetotactic Bacteria by Electron Holography. Science. 1998;282:1868-70.

[98] Yeary LW, Moon J-W, Rawn CJ, Love LJ, Rondinone AJ, Thompson JR, et al. Magnetic properties of bio-synthesized zinc ferrite nanoparticles. Journal of Magnetism and Magnetic Materials. 2011;323:3043-8.

Acknowledgements

I owe my deepest gratitude to my supervisor, Prof. Tatsuo Iwasa, whose encouragement, guidance and support from the initial to the final enabled me to complete PhD research. Most importantly, Prof. Tatsuo Iwasa taught me what the science is and how to do it. I was also deeply impressed by his intelligence and humorous personality from which I always gain lots of energy to continue my work.

I should express my great thanks to Dr. Ken Sawada, Prof. Akira Sakai (Muroran IT), Dr. Shingo Watanabe, Prof. Shuji Ebisu (Muroran IT), Prof. Susumu Chikazawa (Muroran IT), Dr. Kosei Kutsuzawa (Muroran IT) and Dr. Gang Dai (Inner Mongolia Normal University) for their diligent collaborative works. This thesis would not be possible without their collaborative works.

I would like to show my gratitude to Dr. Ken Sawada, Dr. Shingo Watanabe, Dr. Hiromu Sugimoto, Dr. Chaoluomeng, Dr. Li Xing, Dr. Geng Xiong and M.Sc. Wendurige. They gave me a lot of help both in my research work and daily life.

I am grateful of the teachers in foreign exchange center and my Japanese friends. They gave me so many supports in my daily life. With their helps, I made a lot of great memories in Hokkaido. Their civility, politeness and kindness impressed me deeply.

Finally, special thanks to my wife for her understanding, love and support.

Published paper

1. Yiriletu, Tatsuo Iwasa, “Magnetic properties of magnetite synthesized by *Magnetospirillum magnetotacticum* MS-1 cultured at different concentrations of ferric iron” (2015) Biotechnology Letters, vol.37, pp.2427-2433
2. Yiriletu, Shingo Watanabe, Tatsuo Iwasa, “Magnetic bacteria as a tool for bioremediation of heavy metal ion”, Advanced Materials Research (2014) vol. 955-959, pp. 589-592

Conference

1. Yiriyoltu S, Kosei Kutsuzawa, Akira Sakai, Tatsuo Iwasa, “Influence of ferric iron concentrations on the yield and magnetic properties of magnetosome synthesized in *Magnetospirillum Magnetotacticum* MS-1”, the 67th Society for Biotechnology, (2015-10-26~28 Kagoshima, Japan)
2. Yiriyoltu S, Shingo Watanabe, Kosei Kutsuzawa, Tatsuo Iwasa, “The effects of zinc on magnetic properties of the magnetosome in *Magnetospirillum Magnetotacticum* MS-1”, the 66th Society for Biotechnology, (2014-09-09~11 Sapporo, Japan)
3. S. Yiriyoltu, Shingo Watanabe, Tatsuo Iwasa, “Magnetic bacteria as a tool for bioremediation of heavy metal ion”, the 3rd International Conference on Energy and Environmental Protection (ICEEP 2014) (2014-04-26~28 Xi’an, China)
4. S. Yiriyoltu, Shingo Watanabe, Tatsuo Iwasa, “Magnetic properties of

magnetosome formed in *Magnetospirillum Magnetotacticum* (MS-1) cultured with zinc or cobalt", Joint Seminar on Environmental Science and Disaster Mitigation Research 2014, (2014-03-07 Muroran, Japan)

5. Yiriyoltu S, Shingo Watanabe, Kosei Kutsuzawa, Tatsuo Iwasa, "The effects of cobalt-doping on the magnetosome in *Magnetospirillum Magnetotacticum* MS-1", the 65th Society for Biotechnology, (2013-09-18~20 Hiroshima, Japan)
6. S. Yiriyoltu, Shingo Watanabe, Tatsuo Iwasa, "Metal Doping of Magnetic Nano-Particle in *Magnetospirillum magnetotacticum* MS-1", The 7th World Congress on Biomimetics, Artificial Muscles and Nano-Bio, (2013-08-26~30 Jeju Island, South Korea)
7. S. Yiriyoltu, Shingo Watanabe, Tatsuo Iwasa, "Study on the effects of zinc and cobalt on *Magnetospirillum Magnetotacticum* MS-1", Joint Seminar on Environmental Science and Disaster Mitigation Research 2013, (2013-03-08 Muroran, Japan)